CHAPTER FOUR

GEOPHYSICAL INTERPRETATION AND DISCUSSION

4.1. DATA PROCESSING AND INTERPRETATION

4.1.1. Introduction

Processing of potential field data entails the application of various filters to the data in order to accentuate certain chosen features as an aid in the interpretation of the data.

The process of quantitative interpretation of both gravity and magnetic anomalies endeavours to determine a source distribution whose anomalous field matches as closely as possible the actual field on the surface of measurement. The non-uniqueness of the potential field problem results in the introduction of constraints in the form of simplification of geometry, limits to size or depth, range limits on density or susceptibility, or whatever other parameters may seem justified in the context of what is known or can be reasonably inferred about the geologic environment (Paterson and Reeves, 1985).

A short discussion of the effects of the various filters used in the processing of the magnetic and/or gravity data used in this research project follows.

4.1.2. Vertical Derivative

Derivatives tend to sharpen the edges of anomalies and enhance shallow features.
The vertical derivative map is much more responsive to local influences than to broad or regional effects and therefore tends to give sharper picture than the map of the total field

intensity. Thus the smaller anomalies are more readily apparent in area of strong regional disturbances. In fact the first vertical derivative is used to delineate high frequency features more clearly where they are shadowed by large amplitude, low frequency anomalies. From GEOSOFT Inc., 1996;

$$L(r) = r^n$$

with : n = order of differentiation

4.1.3. Analytical signal

This is a filter applied to magnetic data and is aimed at simplifying the fact that magnetic bodies usually have a positive and negative peak associated with it, which in many cases make it difficult to determine the exact location of the causative body.

Nabighian (1972) has shown that for two-dimensional bodies, a bell-shaped symmetrical function can be derived which maximises exactly over the top of the magnetic contact. The three-dimensional case was derived in 1984 also by Nabighian. This function is the amplitude of the analytical signal. The only assumptions made are uniform magnetisation and that the cross section of all causative bodies can be represented by polygons of finite or infinite depth extent. This function and its derivatives are therefore independent of strike, dip, magnetic declination, inclination and remanent magnetism (Debeglia and Corpel, 1997).

The 3-D analytical signal, A, of a potential field anomaly can be defined (Nabighian, 1984)

$$A(x,y) = \left[\frac{\partial M}{\partial x}\right]\hat{x} + \left[\frac{\partial M}{\partial y}\right]\hat{y} + \left[\frac{\partial M}{\partial z}\right]\hat{z}$$

as:

With:

M = Magnetic field.

The analytical signal amplitude can now be calculated (Debeglia and Corpel, 1997) as:

$$/\,A(x,y)\,/ = \sqrt{\left(\frac{\partial M}{\partial x}\right)^2 + \left(\frac{\partial M}{\partial y}\right)^2 + \left(\frac{\partial M}{\partial z}\right)^2}$$

4.1.4. Upward continuation

This is the calculation of the potential field at an elevation higher than that at which the field is measured and is applied to both magnetic and gravity data. The continuation involves the application of Green's theorem and is unique if the field is completely known over the lower surface (which is usually true for gravity and magnetic fields) and where all sources above the lower surface are known (usually all are zero). Upward continuation is used to smooth out near surface effects.

For upward continuation (where z is positive downward) (Telford, 1990)

$$F(x,y,-h) = \frac{h}{2\pi}\iint \frac{F(x,y,0)\partial x \partial y}{\left\{(x-x')^2 + (y-y')^2 + h^2\right\}^{\frac{1}{2}}}$$

Where

F (x', y',-h) = Total field at the point P(x', y',-h) above the surface on which F(x, y,0) is known.

H = elevation above the surface

4.1.5. Downward continuation

Downward continuation is used to enhance features at a specified depth/elevation, lower than the acquisition level. This procedure accentuates near surface anomalies and can be used as an interpretation tool to determine the depth to a causative body. The filter can be

applied to both gravity and magnetic data. Downward continuation is done using the expression (Geosoft Inc., 1996):

$L(r) = e^{hr}$

With h the distance in meters to be continued downward.

4.1.6. Reduction to the magnetic pole

This is a method of removing the dependence of magnetic data on the angle of magnetic inclination. This filter converts data which have been recorded in the inclined earth's magnetic field to what the data would have looked like if the magnetic field had been vertical. A reduction to the pole transform will provide a symmetrical anomaly over a vertically dipping, non-remanent body and is again used as an interpretation aid under certain conditions. At low latitudes, however, an amplitude correction is required to prevent north-south signals from dominating the data. This filter can be described as (Geosoft Inc., 1996):

$$L(\theta) = \frac{1}{[\sin(I_a) + i\cos(I).\cos(D-\theta)]}$$

With:

I geomagnetic inclination

I_a inclination for amplitude correction ($I_a > I$)

D geomagnetic declination

For two-dimensional structures, the anomaly peaks correlate very closely with the analytical signal peaks, indicating that the effect of remanent magnetism is relatively small.

4.2. MAGNETIC DATA PROCESSING AND INTERPRETATION

4.2.1. Introduction

Flight lines ran north-south and interpretation of the data was done in two stages:

- A basic interpretation delineating all major structural features.
- Cross sections along five selected profiles were modeled using 2,5D modeling software.

The basic interpretation was facilitated using the following filtered presentations of the data:

- The total field magnetic contour map, Figure 4.1
- The first vertical derivative contour map, Figure 4.2
- The analytical signal contour map, Figure 4.3
- Upward continued data (to 500m), Figure 4.4
- Upward continued data (to 1000m), Figure 4.5
- Upward continued data (to 2000m), Figure 4.6
- Reduction to the pole, Figure 4.7

4.2.2. Total magnetic intensity contour map

Figure 4.1 is a presentation map that gives the vector sum of all components of the magnetic field. In this study, the remanence observed in the mafic rocks was low and from laboratory determinations do not have any undue influence on the observed magnetic intensity used for the modeling. The total field magnetic contour map reveals the magnetic characteristics of the various lithological units in the study area. Unfortunately, the nature of a magnetic anomaly is a function of the strike of the body. For example, a north-south striking dolerite dyke will have a different associated magnetic anomaly than the same dyke striking east-west. The total field magnetic contour map is consequently primarily used to identify various lithologies.

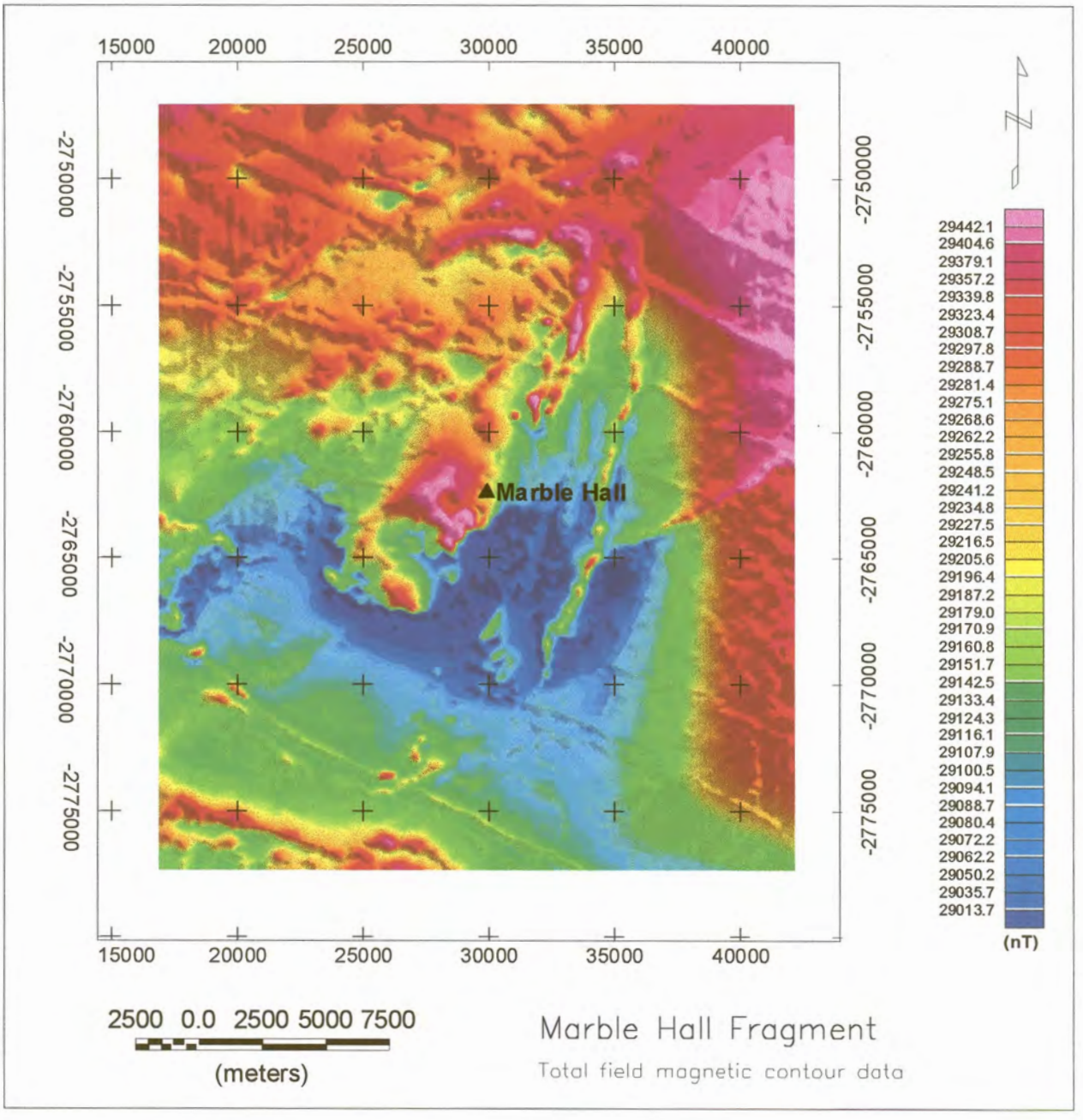

Figure 4.1 Total field magnetic colour contour data

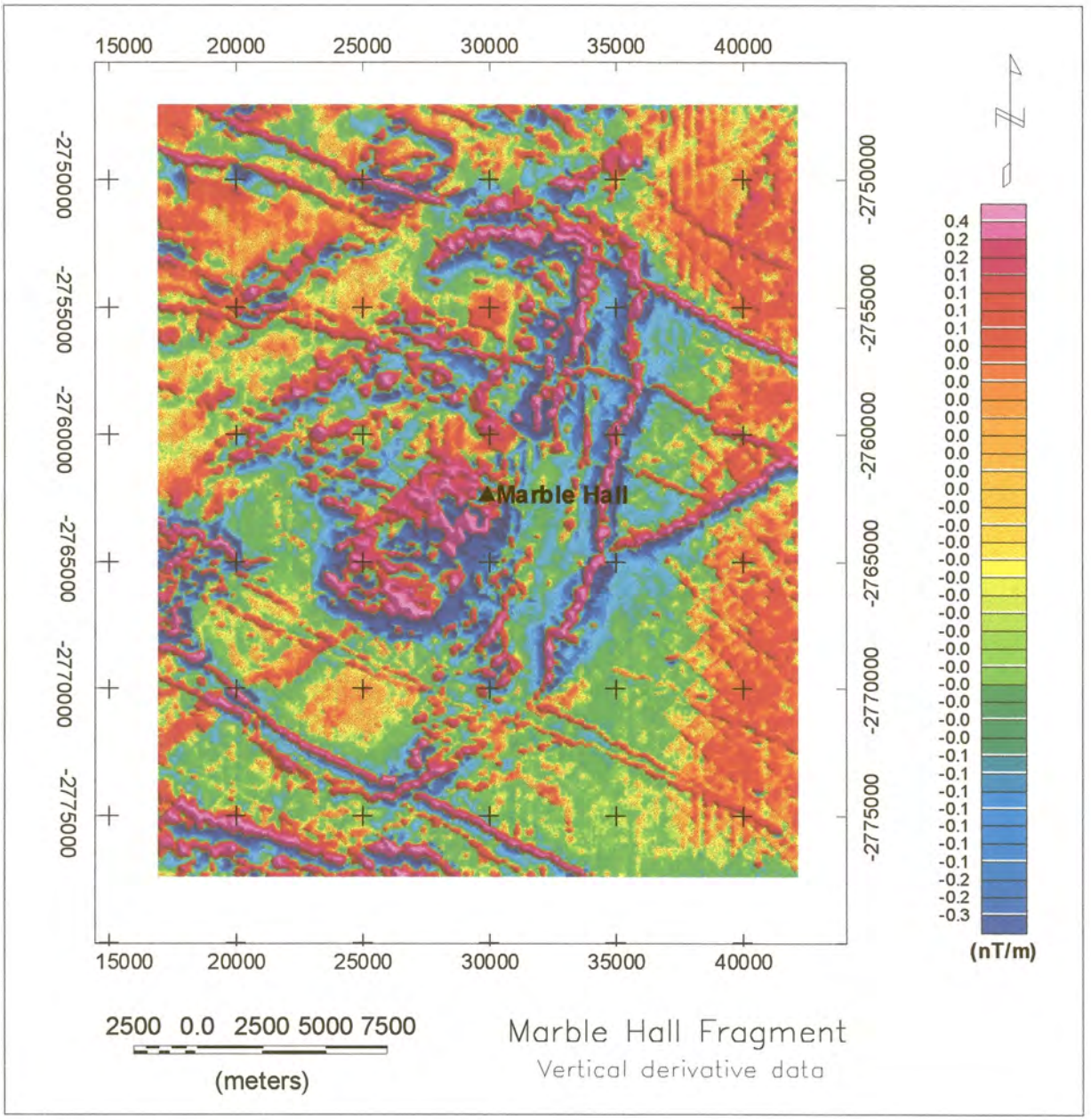

Figure 4.2. First vertical derivative

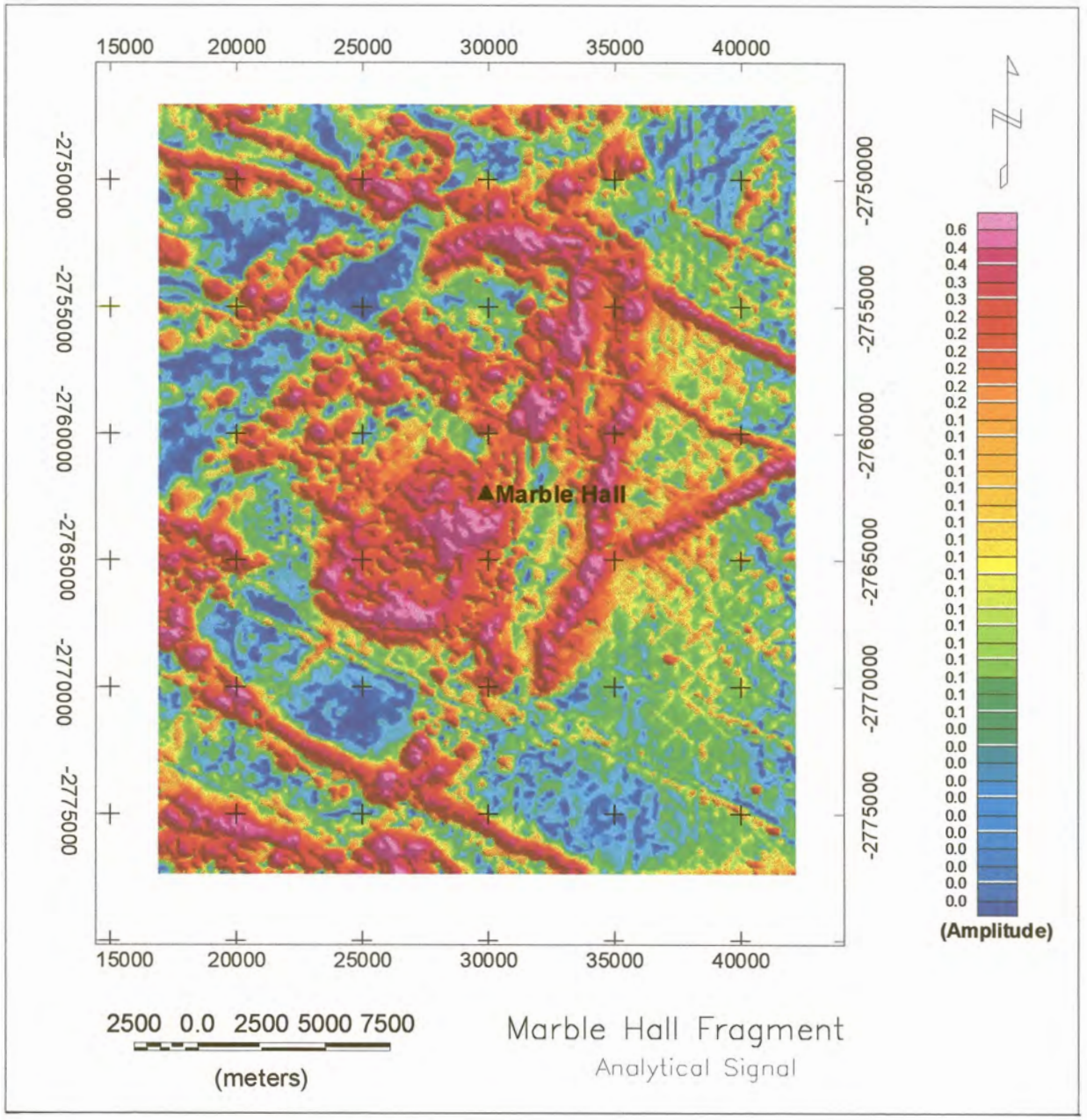

Figure 4.3. Analytical signal

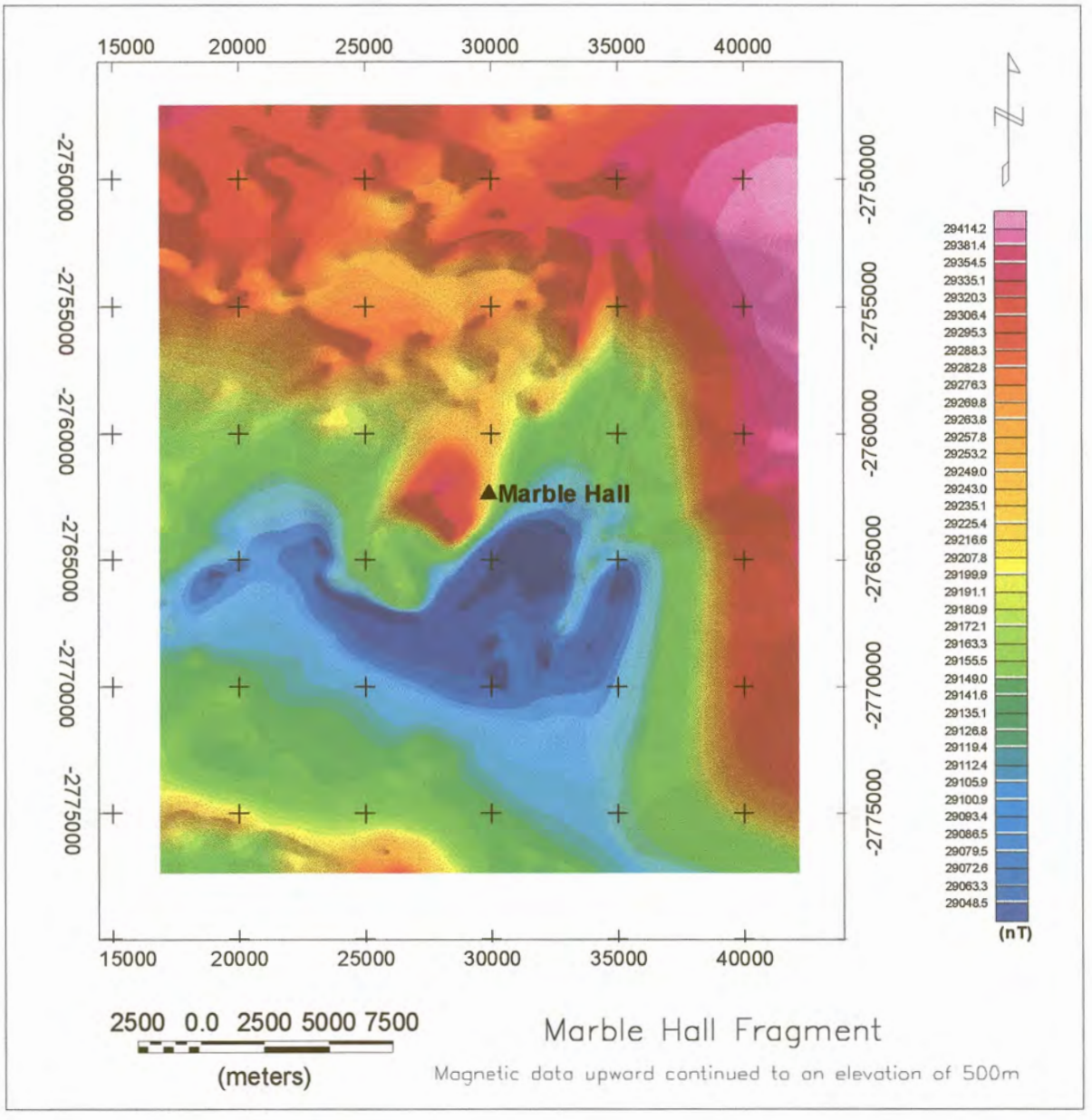

Figure 4.4. Magnetic data upward continued to an elevation of 500m

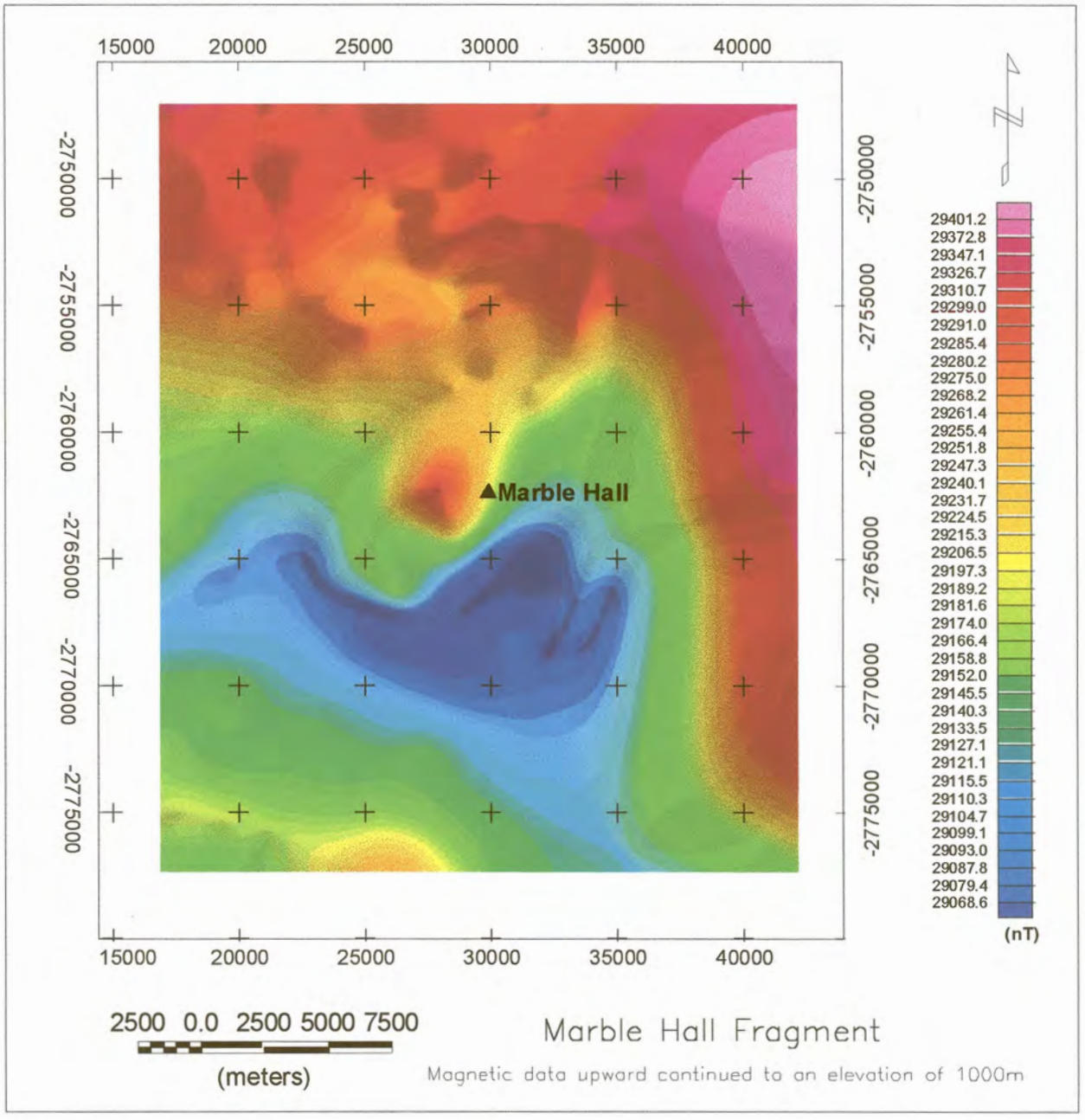

Figure 4.5. Magnetic data upward continued to an elevation of 1000 metres

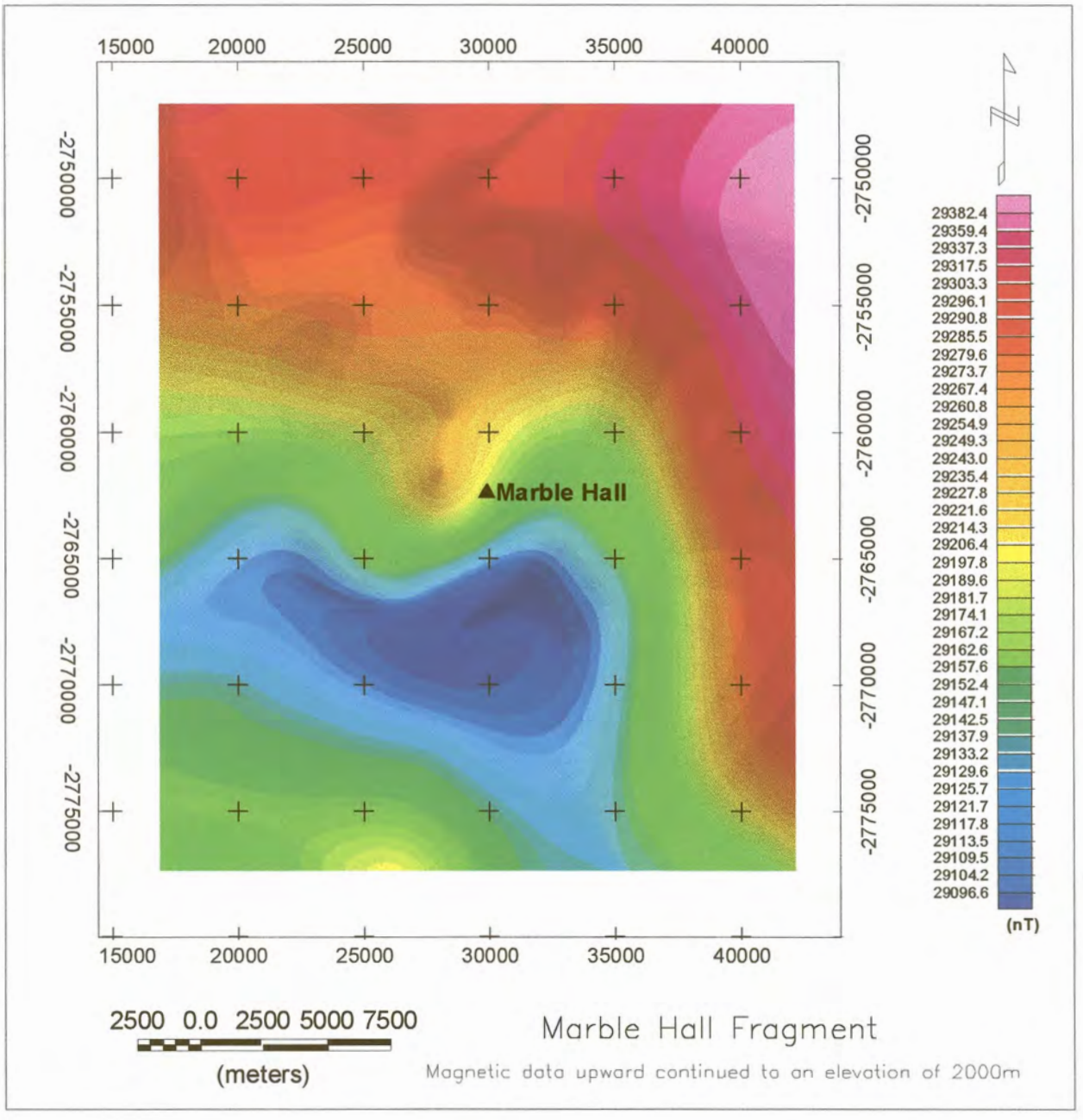

Figure 4.6 Magnetic data upward continued to an elevation of 2000 metres

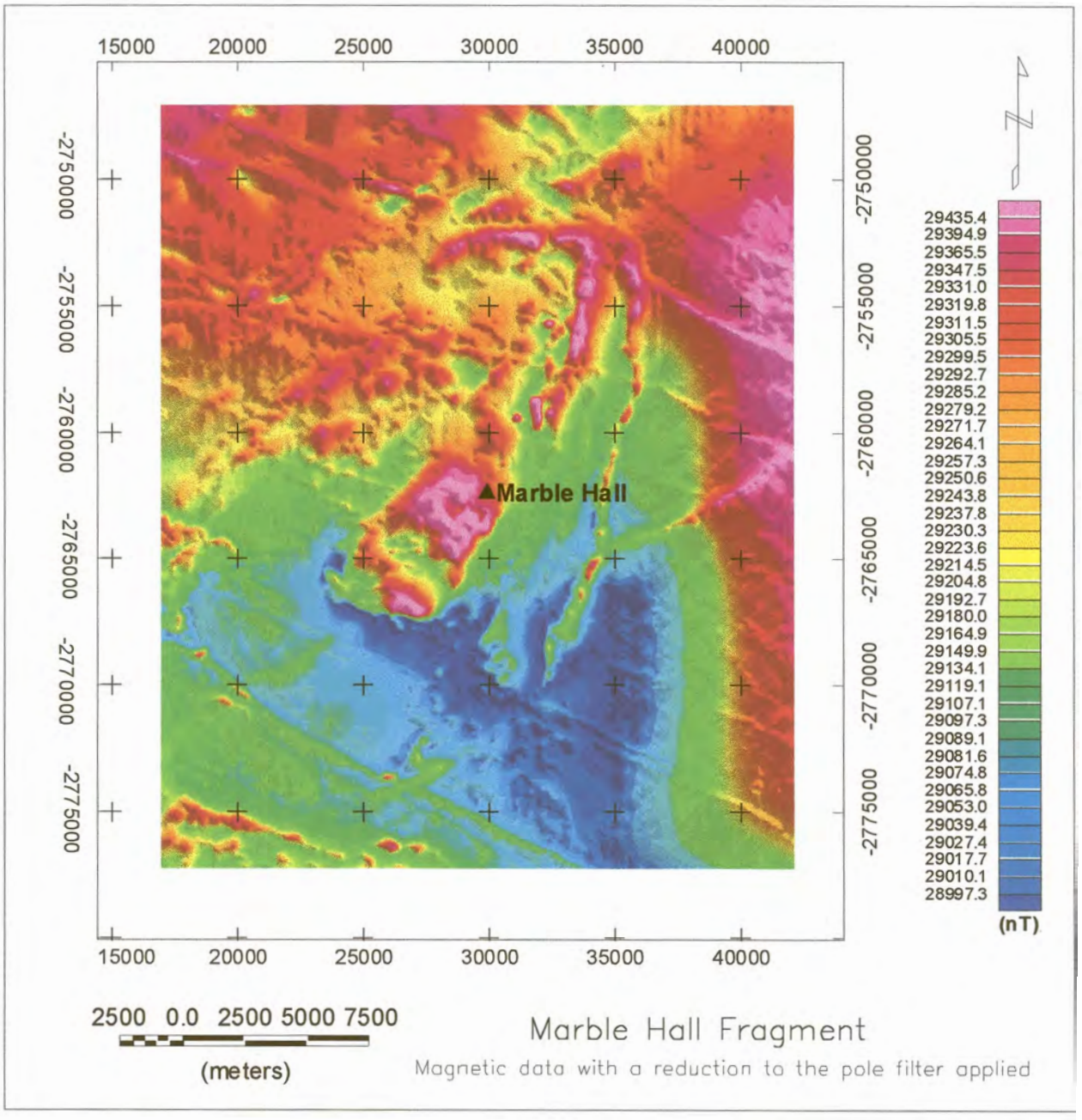

Figure 4.7 Magnetic data with a reduction to the pole filter applied

4.2.3. Vertical Derivative map

Comparison of the vertical derivative map (Figure 4.2), with the total field map (Figure 4.1), shows a marked increase in 'visibility' of structural features, especially in the southern part of the study area.

4.2.4. Analytical signal

This filter was applied to the airborne total magnetic field data. Comparing this map (Figure 4.3), with the total field magnetic contours (Figure 4.1), the difference is immediately obvious along the edges of the dolerite dyke in the south-west and the central portion of the Swartkop Marble Hall anticline. The analytical signal amplitude maximises over the edge of the magnetic structures. This map was used to delineate the edges of lithological units and to determine the centres of two-dimensional structural features.

4.2.5. Upward continuation

The total field data was upward continued to 500m (Figure 4.4), 1000m (Figure 4.5) and 2000m (Figure 4.6). Upward continuation to 500m did not have a significant effect on the original total field data. Upward continuation to 1000m did however have a significant filtering effect leaving only the fold closure of the Swartkop Marble Hall Anticline to the north, the magnetic highs at the central portion and the north-south lineament towards the eastern boundary. Upward continuation to 2000m reveals a marked distinction between any of the other upward continued data and the original data, in that the fold closures are no longer apparent and the magnetic high at the central part has disappeared leaving just a faint

outline. Also, the north south lineament to the eastern boundary is better defined, the magnetic low to the south of Marble Hall is more pronounced, and, finally, the highest magnetic signature (pink) is more confined to the extreme north eastern border.

4.2.6. Reduction to the Pole (RTP)

The reduction to the pole transform (Figure 4.7), resembles to a large extent the total field data except in the west where the Wonderkop fault appears to be better defined. In the northern part of the fragment where the faulting on the fold also seems to be better defined which would indicate that the influence of magnetic data on the angle of magnetic inclination has been removed. Thus, in removing the anomaly asymmetry caused by the magnetic inclination, the anomalies are better located relative to the causative bodies.

4.3. Processing of gravity data

4.3.1. Reduction to Bouguer values

Processing of the data to obtain the Bouguer values was done using the Oasis Montaj software from GEOSOFT. First, the base station at Marble Hall was tied in to the absolute values known for the station at Groblersdal. Second, the other base station values were tied in to the absolute value calculated for the station at Marble Hall. These base stations were then tied to the International Gravity Standardisation Network values (Morelli et al., 1974) and were referred to the gravity formula based on the 1967 Geodetic Reference System (Moritz, 1968). Terrain corrections were not applied since the main area of interest for this research was fairly flat as is evident from the elevation contour map given in Figure 4.8. The Bouguer gravity map is shown in Figure 4.9.

4.4. Interpretation of potential field data

4.4.1. General

The interpretation of the data was done in three stages. These consisted of:

- Correlating geological units with features identified on the magnetic and gravity contour maps.
- Do a structural interpretation of the magnetic and gravity contour maps.
- Do a vertical profile interpretation along a number of profiles across the study area.

4.4.2. Correlate known geology with observed geophysical anomalies.

In the first stage a simplified outline of the geology was superimposed onto:

- the total field airborne magnetic data downward continued to ground level (Figure 4.10),
- the vertical derivative of the magnetic data (Figure 4.11),
- the bouguer gravity map (Figure 4.12),
- the bouguer gravity map with contour lines, emphasising the steepness of gradients in certain areas (Figure 4.13).

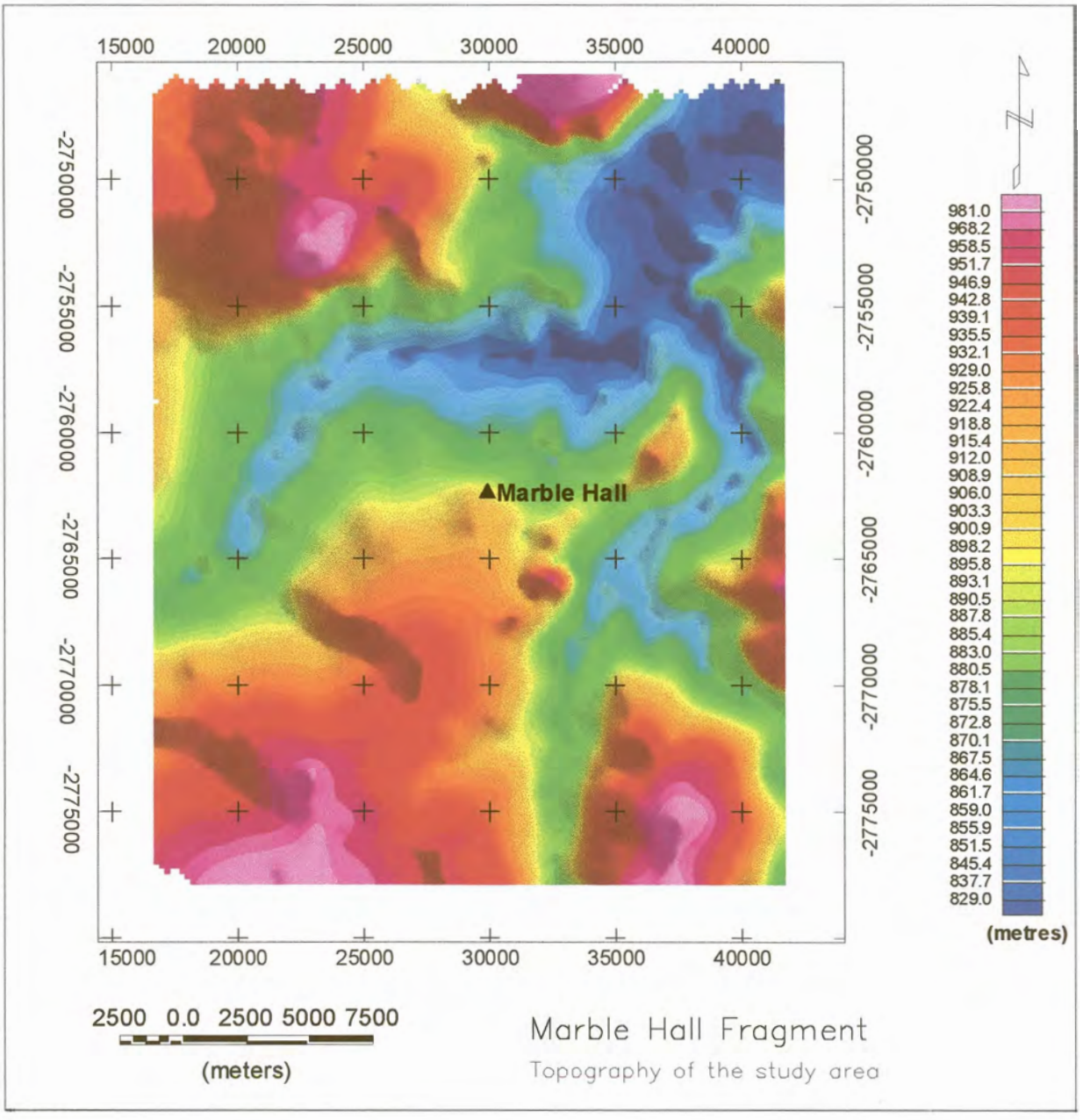

Figure 4.8. Topography of the study area

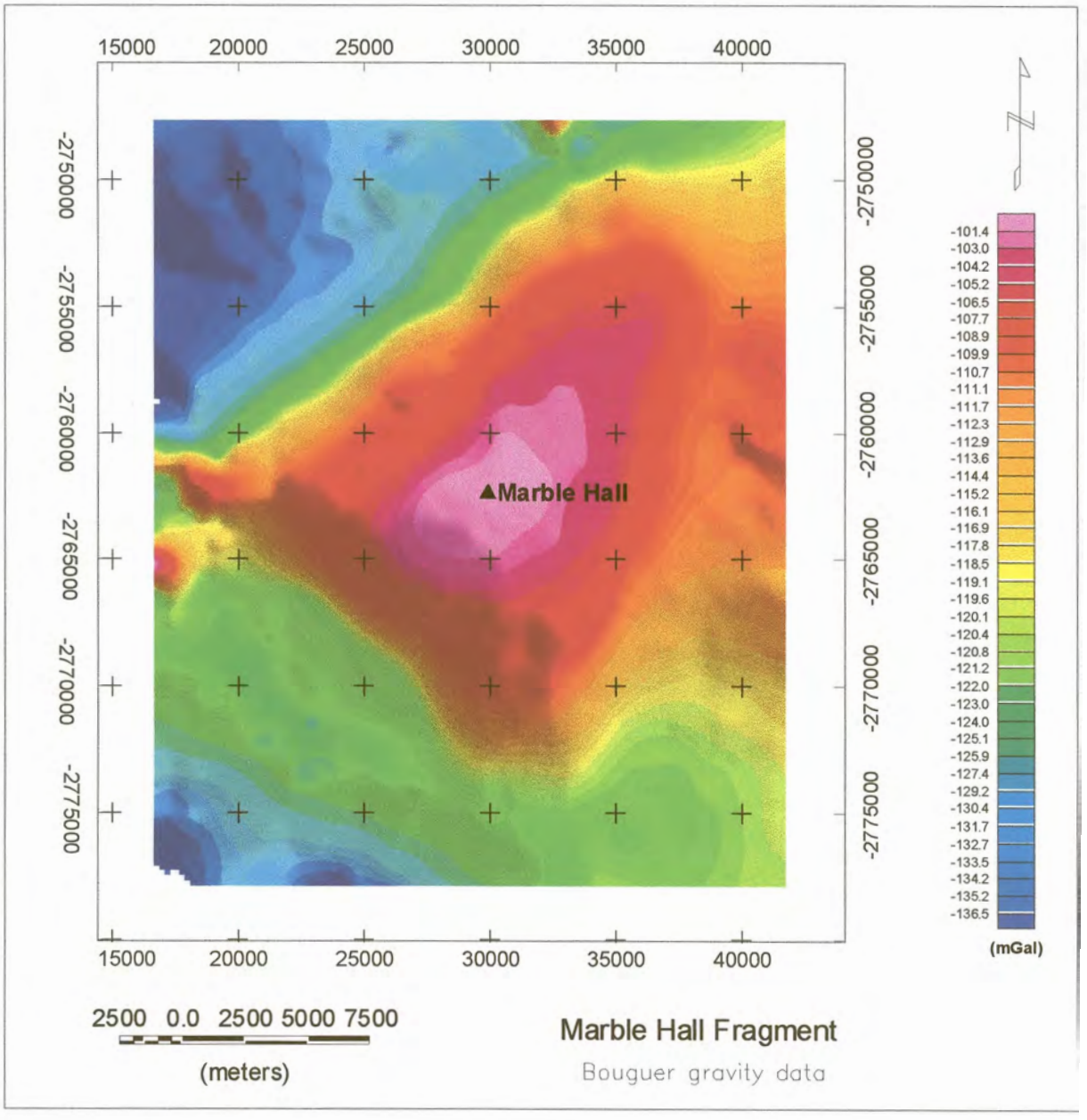

Figure 4.9 Bouguer gravity map

These maps were used to tie the geophysical data to known geological units and features. The following units and features have been identified and the following numbers allocated.

1. Pretoria Series
2. Makeckaan Formation
3. Malmani dolomite
4. Karoo Supergroup
5. Elandslaagte Dome (Archaean rocks)
6. Wonderkop fault
7. Faults
8. Nebo Granite
9. Karro dolerite sills
10. Archaean rocks of the Moos River Fragment
11. Diorite
12. Dyke
13. Fold

To futher facilitate the interpretation of the gravity map, the actual contour lines (Figure 4.13), were included on the colour coded gravity map. This gives a better visualization of the gradient in the observed gravity values.

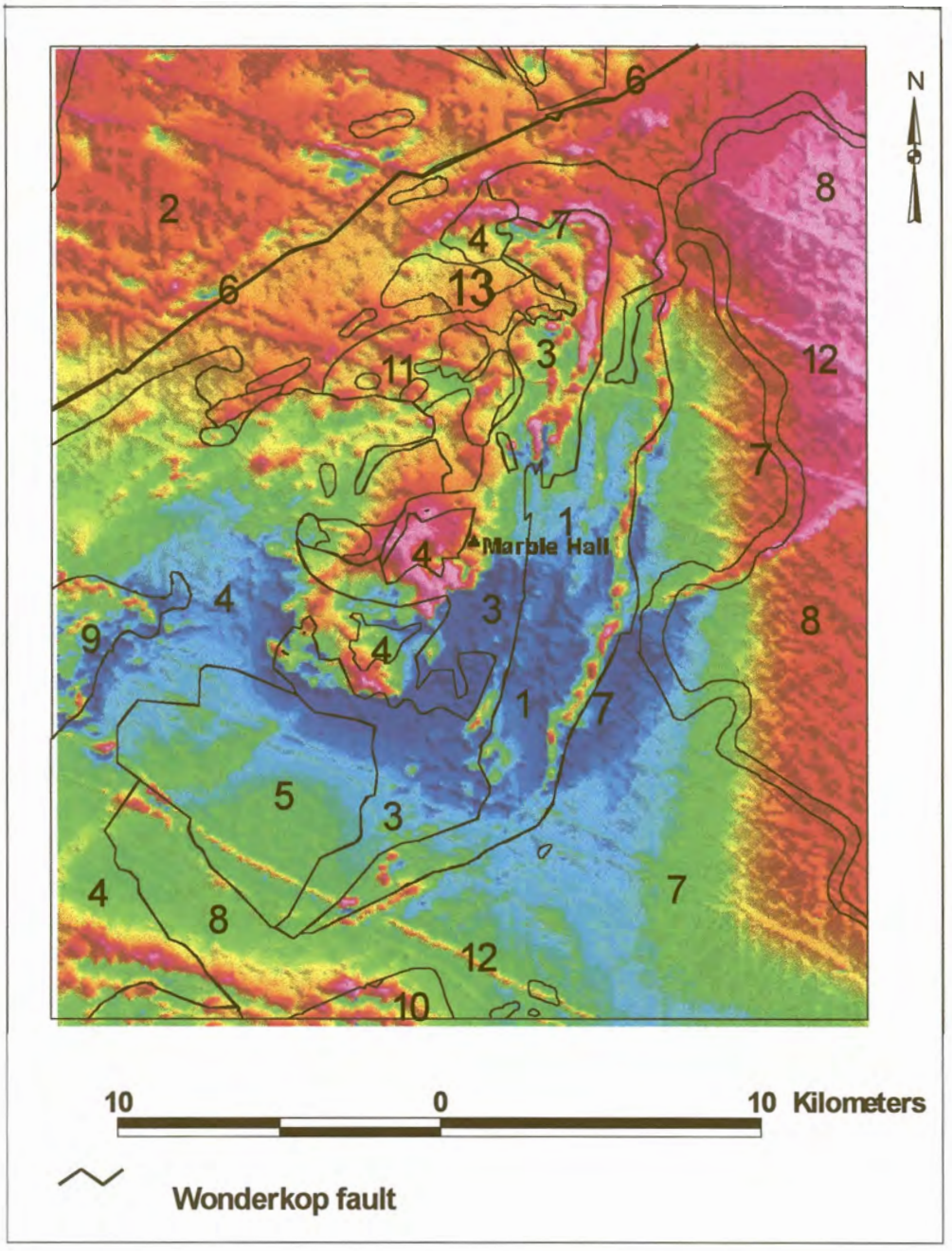

Figure 4.10. Simplified outline of geology superimposed on downward continued total field magnetic data

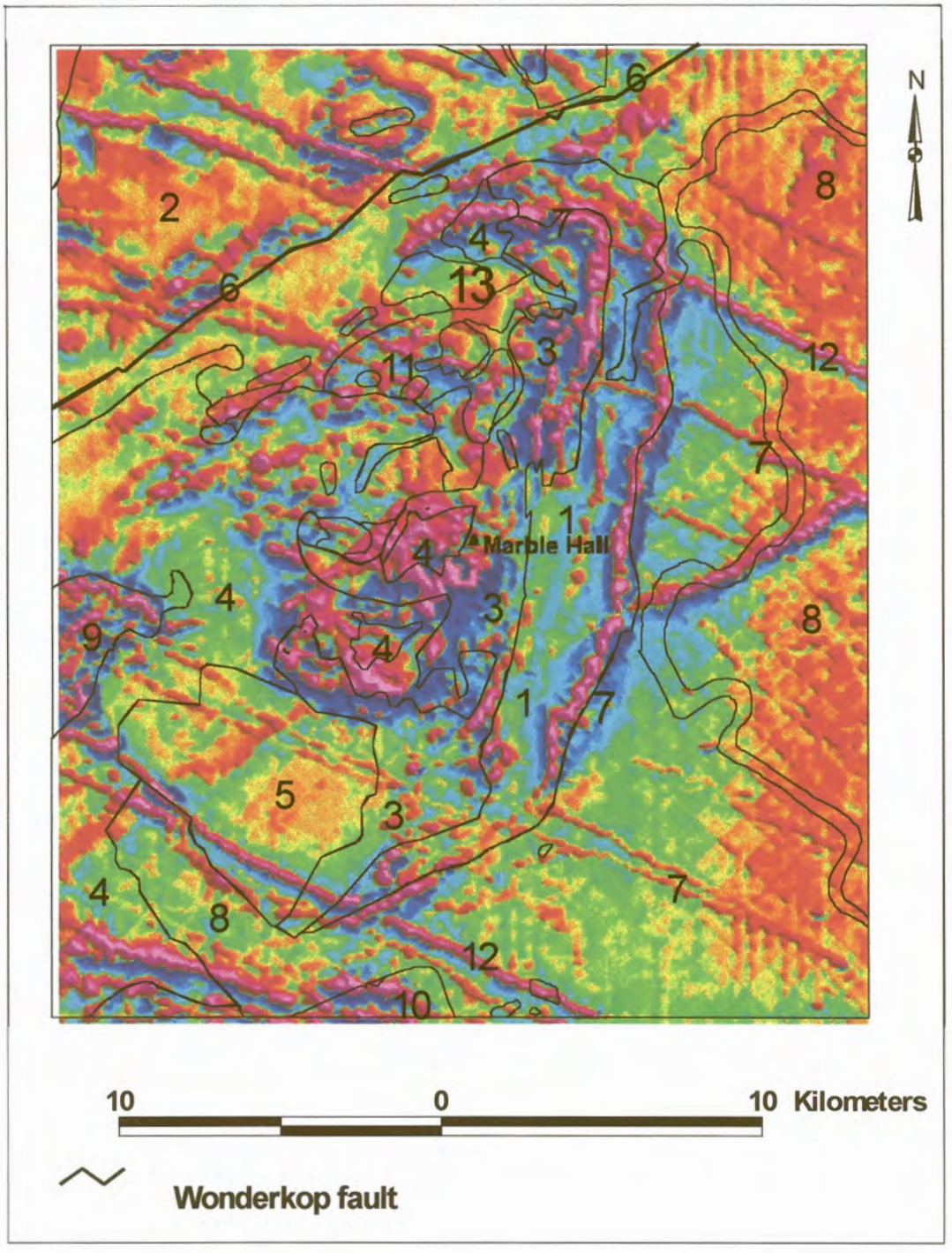

Figure 4.11. Features identified from the correlation of vertical derivative map with simplified geology

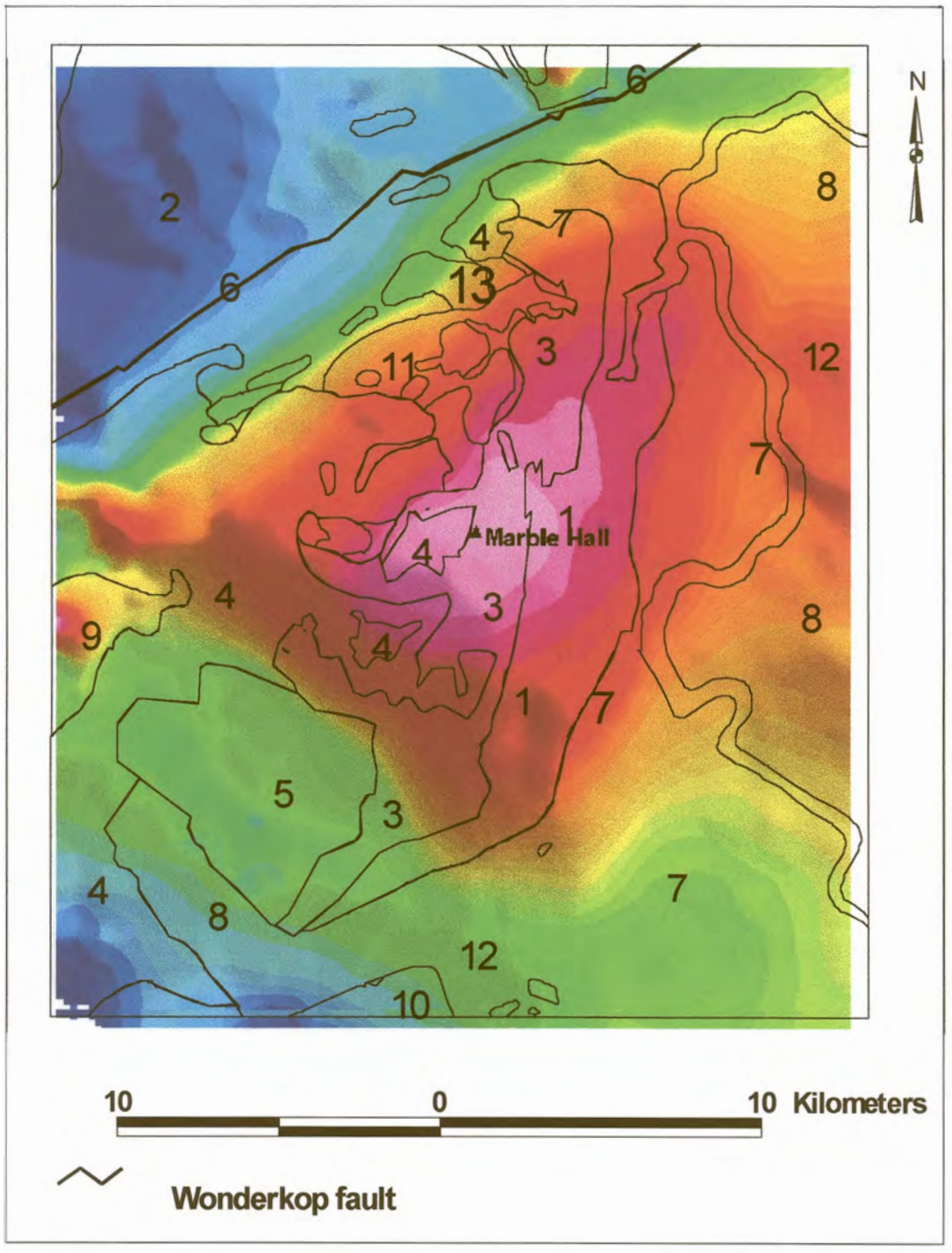

Figure 4.12. Bouguer gravity map with outline of simplified geology

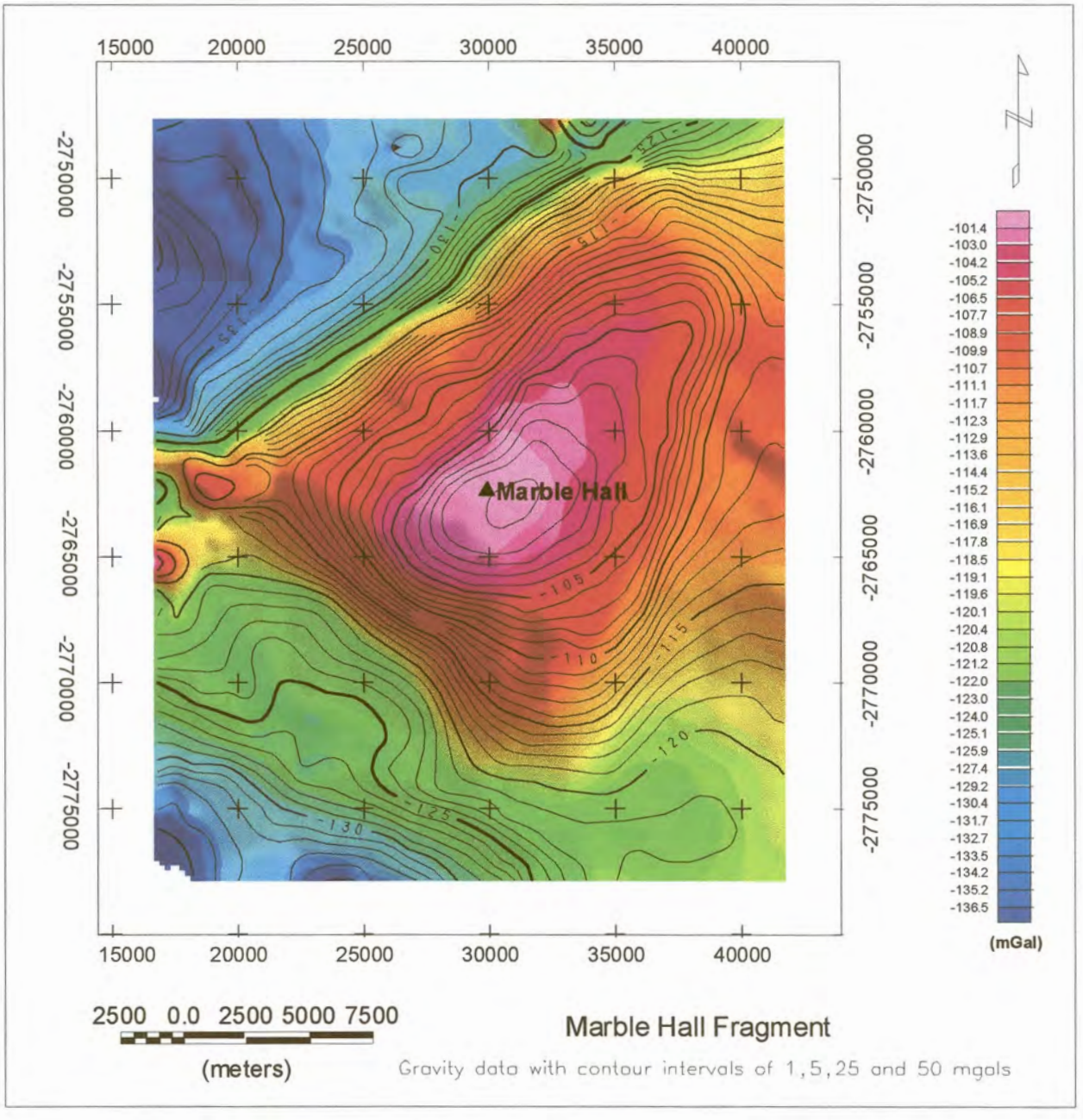

Figure 4.13: Bouguer gravity map with contour lines to emphasise the steepness of the gradient in some areas.

4.4.3. Structural interpretation of magnetic and gravity contour maps.

4.4.3.1. Gravity

There is a good measure of correlation between several of the mapped geological features and the observed gravity values. The very large anomaly has a shape which roughly follows the northeast-southwest trend of the Fragment. The maximum amplitude of the gravity high is in the order of 30 mgal. This is too high to relate to either the surface geology or the topography of the area. .

The steep gravity gradient observed in the north-western corner (Figure 4.13), is interpreted as a fault controlled contact between two lithologies. The interpreted fault trends from the western boundary to the northeast at a strike angle of approximately 45 degrees and is interpreted as the Wonderkop fault delineated by Lee and Sharpe (1983) and many others.

The gravity data suggest the presence of high density rocks at the centre of the Marble Hall Fragment. This gravity high is situated between the prominent Wonderkop fault to the west and a suspected north-south trending fault to the east (see next section).

Though the Marble Hall Fragment is bordered to the east and north-east by the Bushveld Complex granite, both the magnetic and gravity data associated with the eastern and north-eastern parts of the Fragment suggest that the Bushveld granite in these areas is underlain by relatively thick mafic rocks at great depth.

4.4.3.2. Magnetics

To correlate observed magnetic features with topography, the magnetic data were draped over the topography using ERMapper software. The Wonderkop fault and an interpreted north-south fault are shown in Figure 4.14.

A large number of dykes and faults have been identified using the various filtered airborne magnetic contour maps. These features are shown in Figure 4.15. In this figure, feature 1 is identified as the Wonderkop fault, while feature 2 is interpreted as the major north-south trending fault. This fault has no surface geological expression.

4.4.4. 2.5D modeling of selected profiles.

Initially three east-west striking profiles were selected on both the total field magnetic data as well as the gravity data. These lines are labeled AA', BB', and CC' in Figures 4.16(a) and (b), where the relative positions of the profiles are indicated.

The software used for the interpretation of the data is MAGIXP (MAGIX^{PLUS}) which is an interactive, graphically oriented, modeling program designed for the interpretation of gravity and magnetic data (potential field data).

For the magnetic data, the magnetic susceptibility value for the background and each body comprising the model is expressed in SI units. A magnetic inclination and declination of -60^0 and -17^0 respectively were used. The susceptibilities used for the various lithological units are given in Table 7.

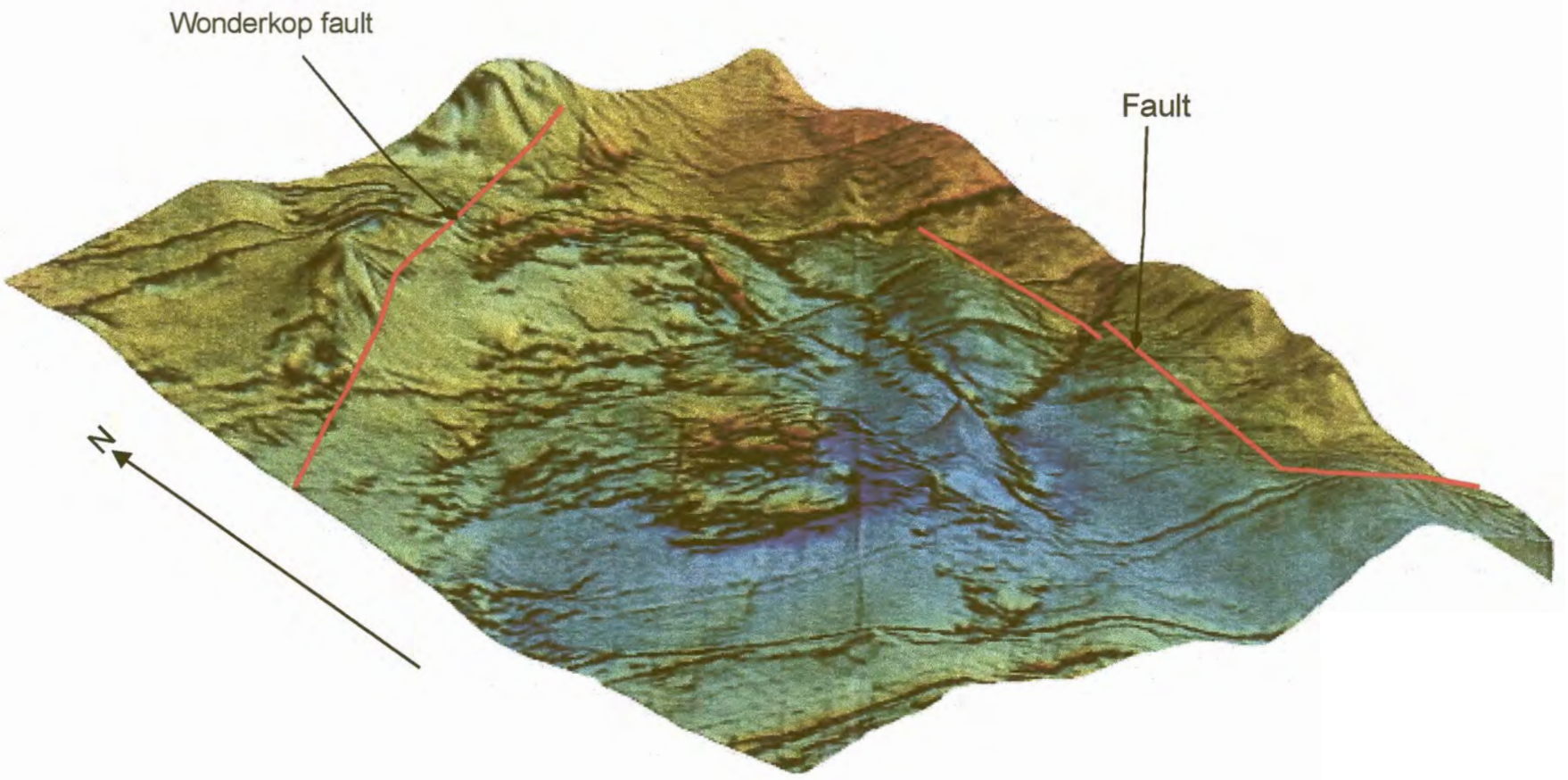

Figure 4.14. Total field magnetic data draped over the topography

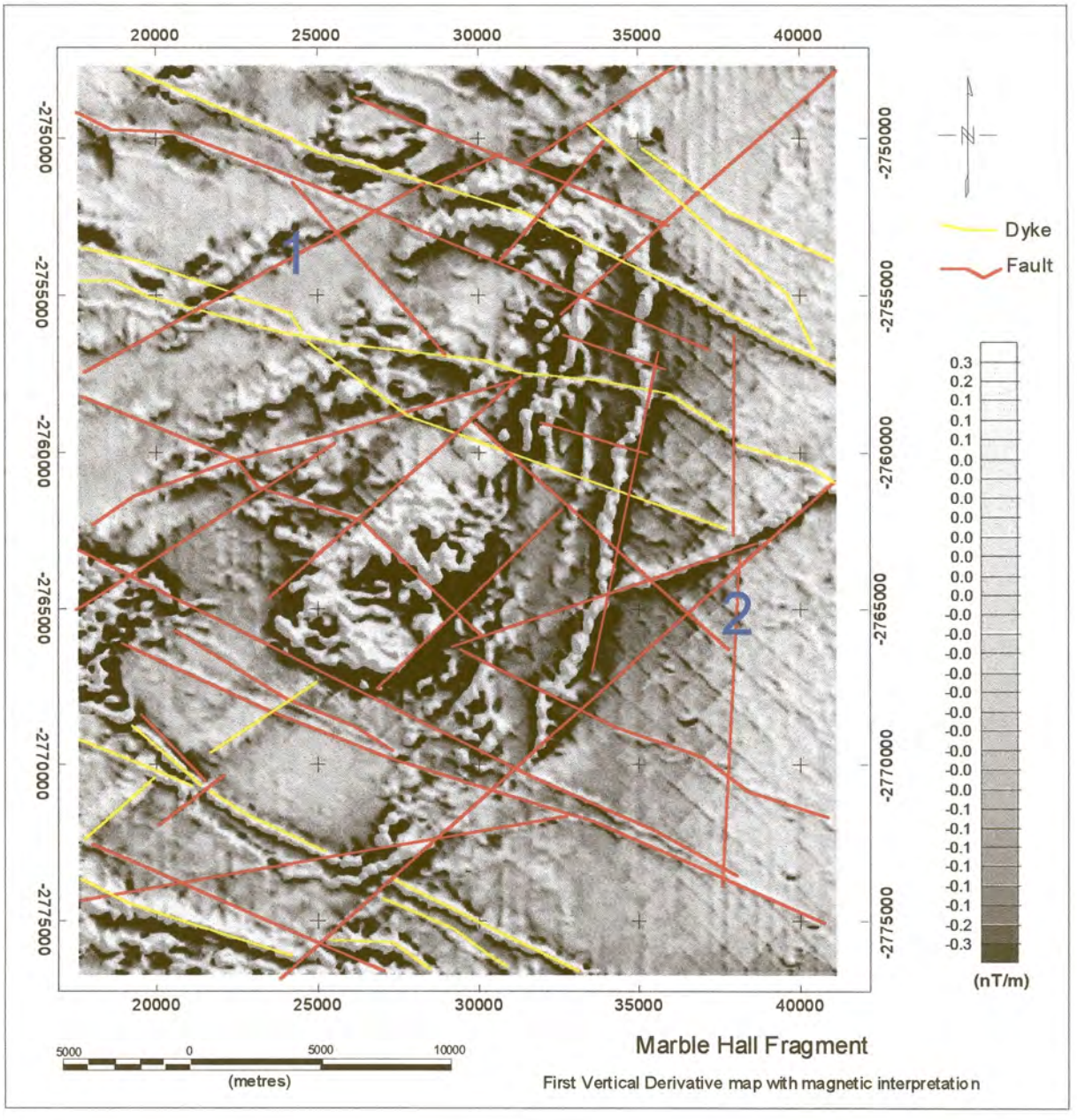

Figure 4.15. Interpreted structures from the vertical derivative map (grey scale)

A prominent magnetic signature with an amplitude in the order of 290 nT is observed in the centre of the Fragment, in about the same position as the gravity high. This anomaly remains prominent even when the data are upward continued to a height of 2000m, (Figure 4.6).

The KT-9 Kappmeter (susceptibility meter) supplied by the Council for Geoscience was used in determining the magnetic sucseptibility of outcrops. Laboratory determination at the Council for Geoscience, of susceptibilities of rock samples taken from the few exposed outcrops, mostly granites and Transvaal Supergroup rocks , revealed that the samples were not remanently magnetised.

Hattingh (1991), however, described the dominance of remanent magnetism in all the structural mafic zones of the Bushveld Complex, except the weakly magnetic Critical Zone. The Main Zone has a low susceptibility despite having a high natural remanent magnetism (NRM) because the carriers of magnetisation are single domain grains which are very small with little or no contribution to the susceptibility of the rock unit (Hattingh, 1986b). Larger magnetic grains which can support higher susceptibilities are very scarce or in many cases absent Hattingh (1986a, b).

Hattingh (1989, 1991), indicated that the NRM in the Upper Zone is nearly 200% larger than the induced magnetisation and assumed that 80% of the NRM of the Upper Zone consist of random secondary magnetisation. This, according to Hattingh (1991), reflects that for the interpretation of magnetic anomalies associated with this zone, the induced component of the anomaly is more important than the permanent remanent magnetisation of the Upper Zone.

The susceptibilities of the Upper and Main Zones used in the modeling were taken from Hattingh (1991). Table 7 shows the susceptibilities of the various rock units.

Table 7: Susceptibilities used for rocks in the research area.

Rock Formation		Susceptibility (SI units)
Makeckaan Formation		0,003
Nebo Granite		0,002
Pretoria Group		0,003
Dolomite		0,000
Bushveld basic rocks	Upper zone	0,11129
	Main Zone	0,0025
Bloempoort Formation		0,000
Archaean Granite		0,000

The regional was estimated for the magnetic profiles by fitting a second order polynomial to the TMI contour map. For the gravity data a straight or very slow curving datum line, was subtracted from the data.

Starter models representing the structure of the Marble Hall Fragment as interpreted from surface geological mapping and excluding, on purpose, the mafic rocks known to exist in the central part of the Fragment, were used. The topography along these profiles are given in Figure 4.17. The gravity and magnetic data and the various geological cross sections are given in Figure 4.18 (a) and (b) for profiles AA', BB' and CC' respectively.

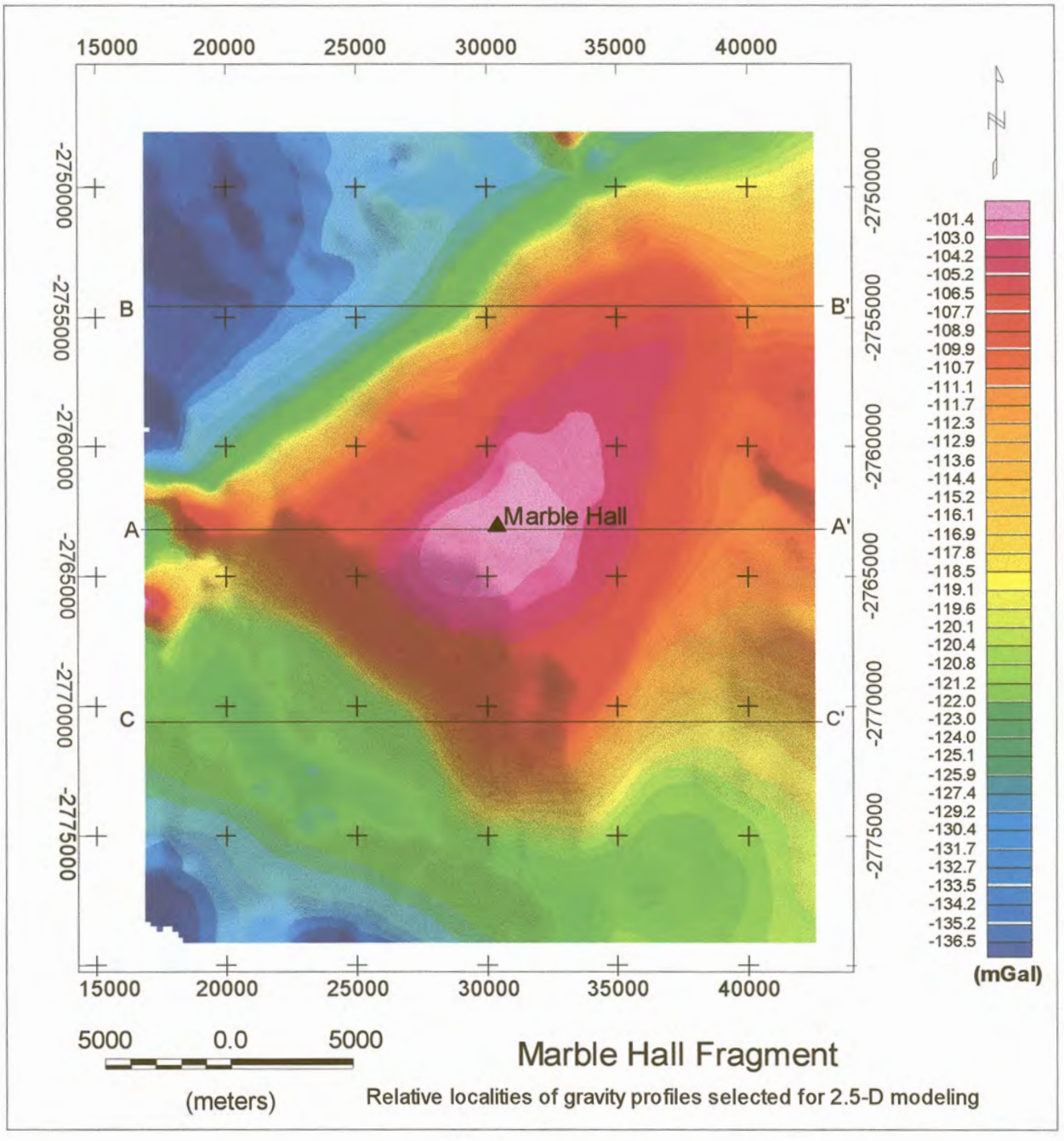

Figure 4.16a : Relative locality of gravity profiles selected for 2.5-D modeling

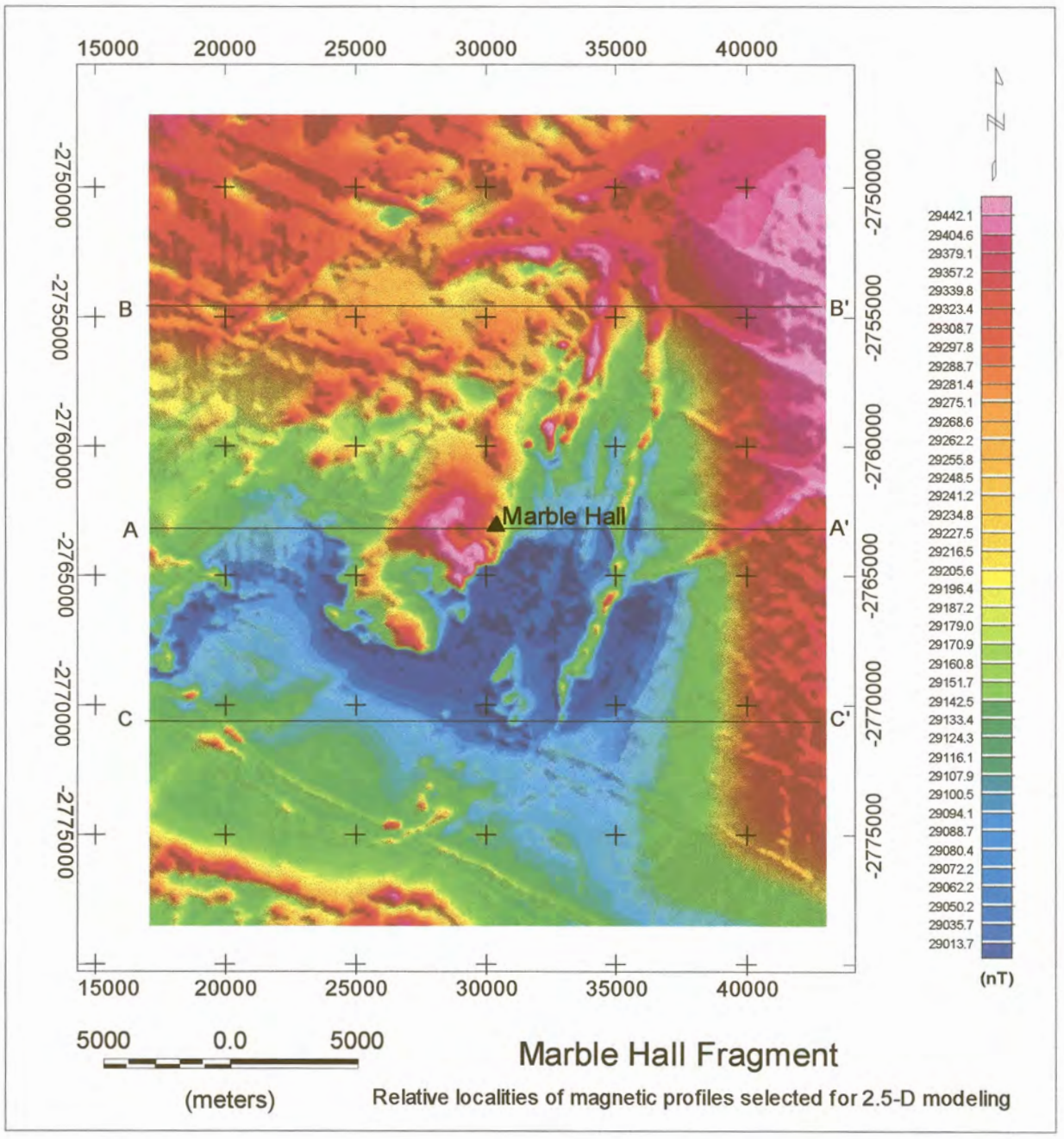

Figure 4.16b: Relative locality of magnetic profiles selected for 2.5-D modeling

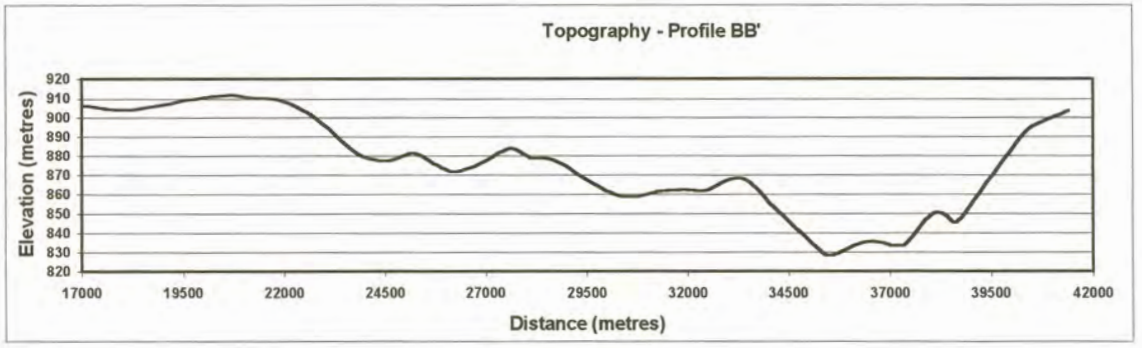

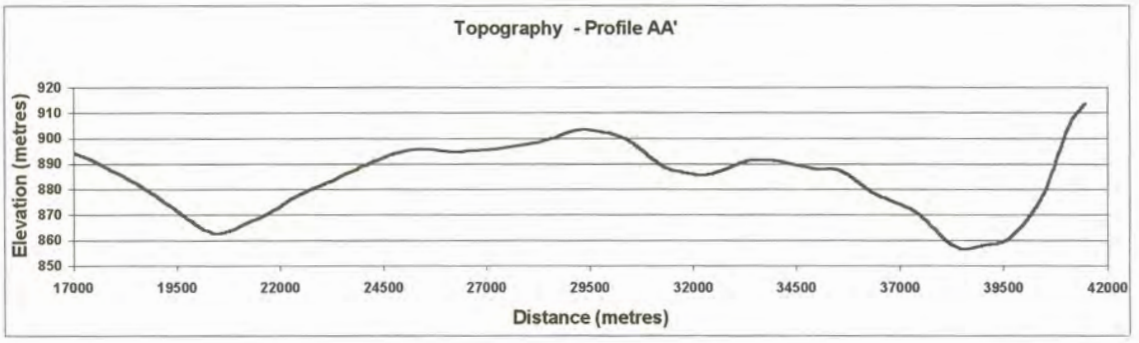

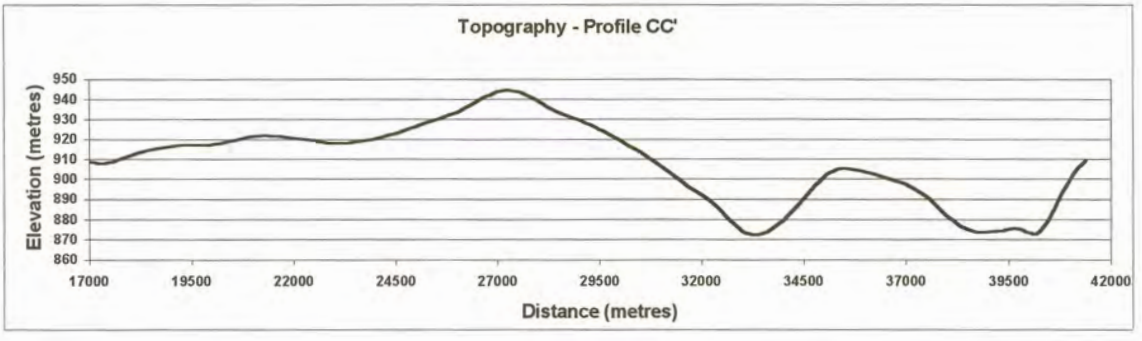

Figure 4.17: Topographic relief along profiles AA', BB' and CC'

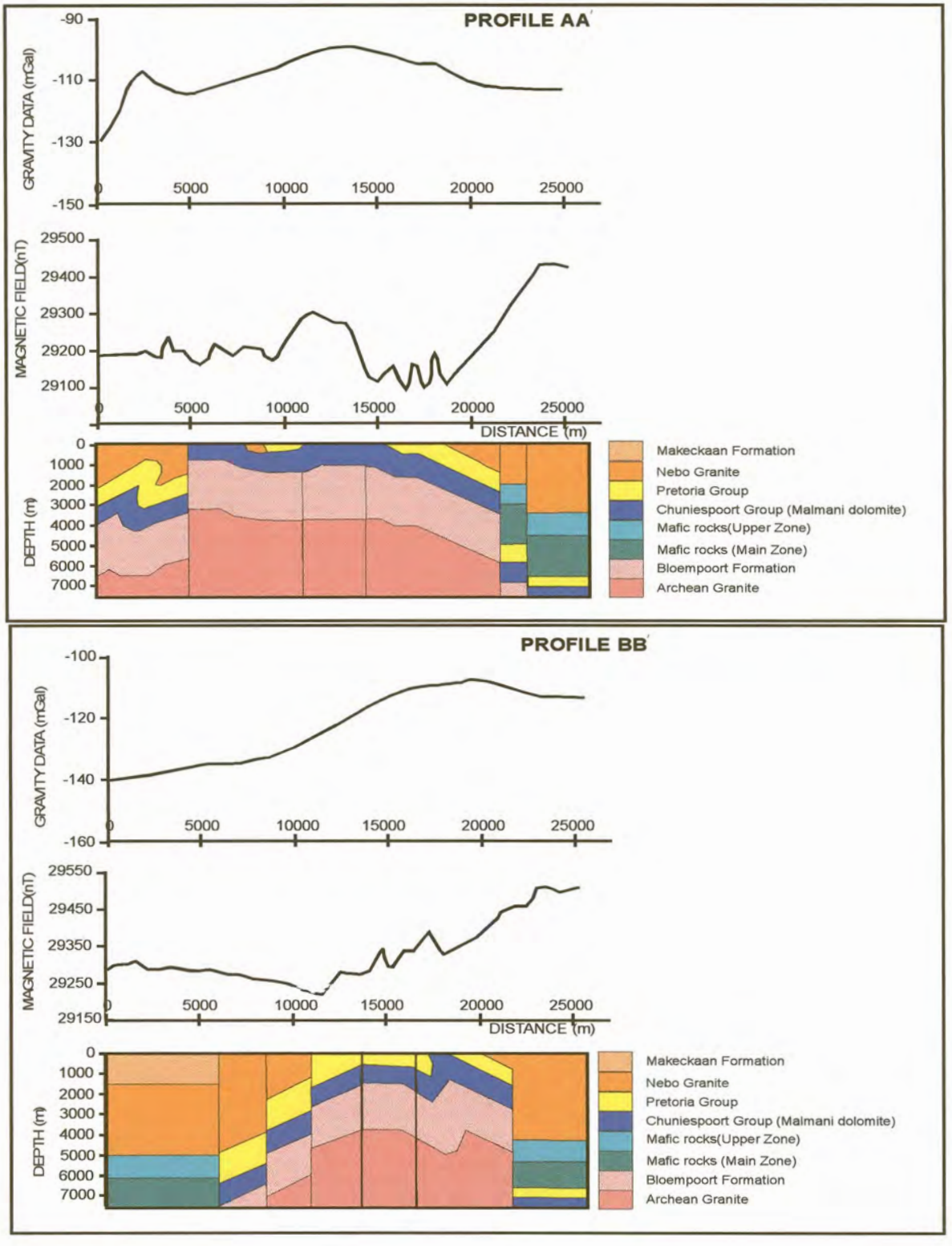

Figure 4.18 (a). Starting models for profiles AA' and BB' respectively.

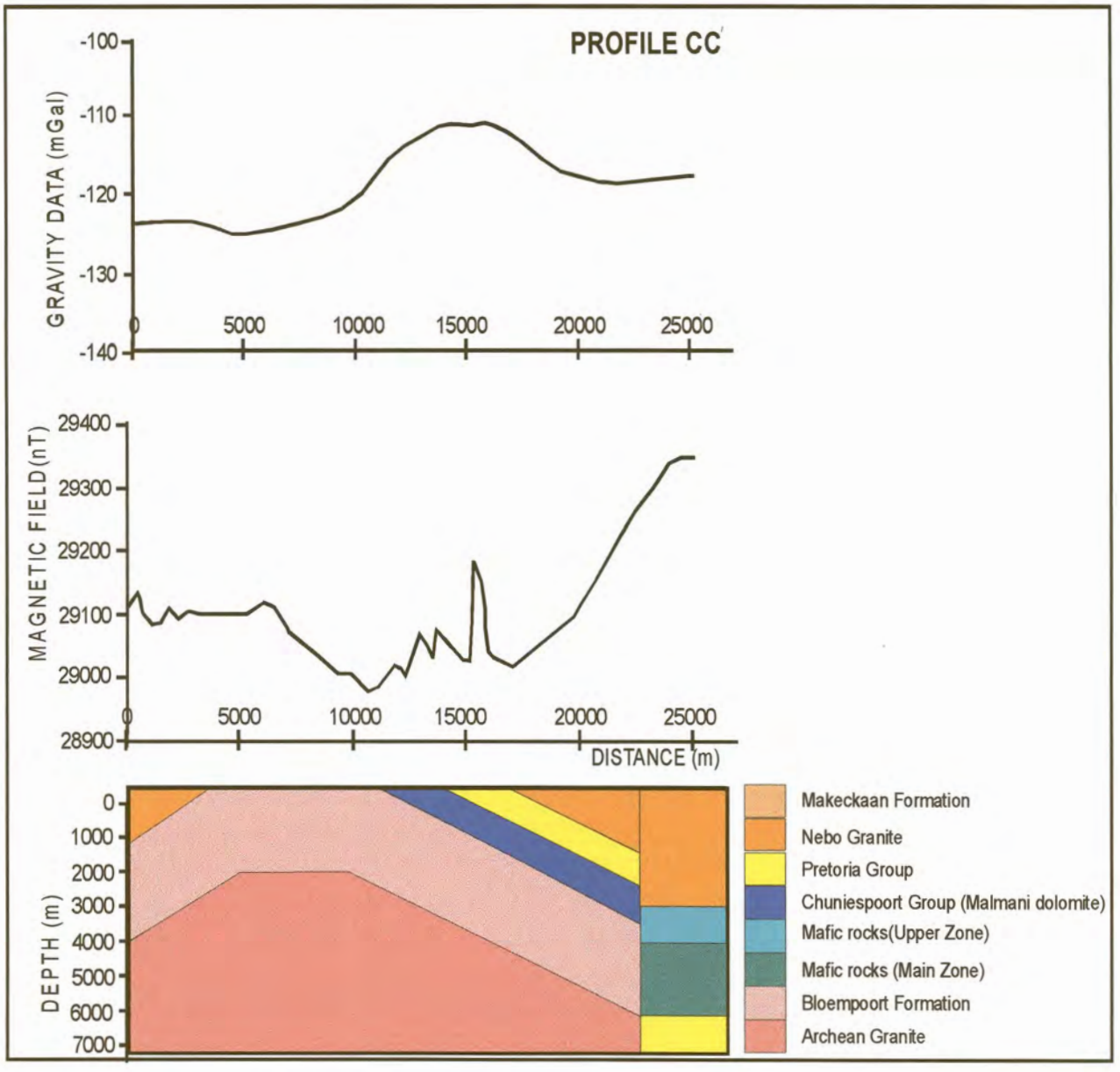

Figure 4.18b. Starting model for profile CC'

The geological models in Figures 4.18 (a) and (b), were then adjusted to fit the potential field data. The final geophysical models are given in Figures 4.19 (a) and (b).

Based on the interpreted profiles AA', BB', CC', Figures 4.19 (a),(b) and (c), it is possible to get an idea of the strike of the intrusive body. In order to confirm its linear trend and perhaps, the width, profiles DD' and EE' along the suspected strike and at right angle to the strike respectively, were drawn for modeling (Figures 4.20 (a) and (b)).

The geological cross-sections (Figure 4.21) along the profiles were used as starter models for profiles DD' and EE'. Again, the existence of mafic rocks in the central part of the Fragment is ignored in these profiles. The final geophysical models are given in Figures 4.22 and 4.23.

It is worthy of note that in the final geophysical models presented (Figures 4.19(a),(b), (c), 4.22 and 4.23), for the gravity models, background refers to Archaean Granite with a density of 2.67 g/cm^3, while for the magnetic models, background refers to a combination of Archaean Granite, Malmani dolomite and the Bloempoort Formation as single model units, having magnetic susceptibilities of zero.

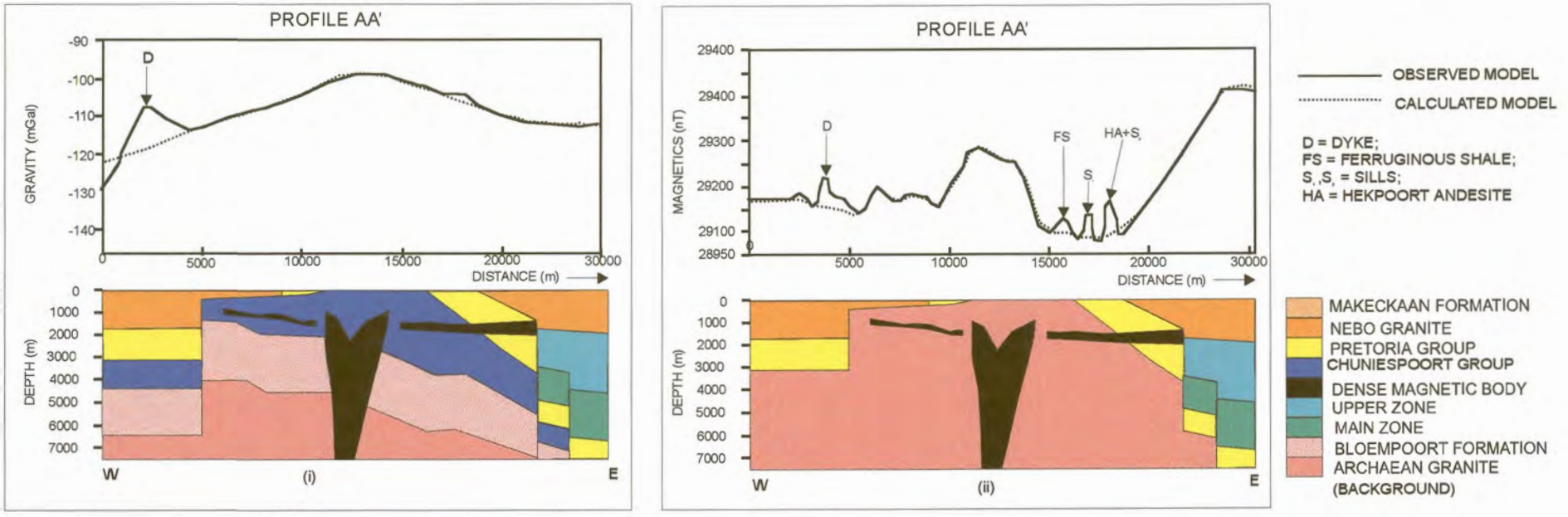

Figure 4.19a : Geophysical models for profiles AA$'$ (i) the gravity and (ii) the magnetics

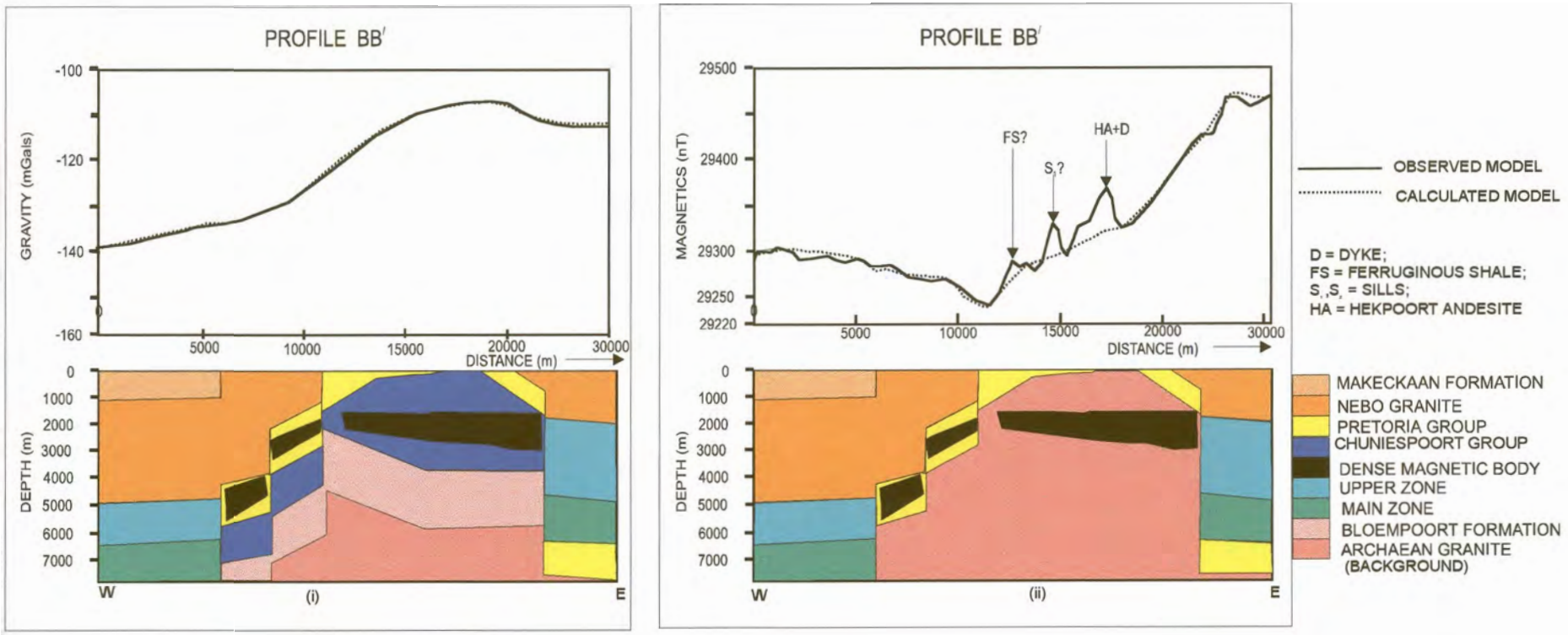

Figure 4.19b : Geophysical models for profiles BB' (i) the gravity and (ii) the magnetics

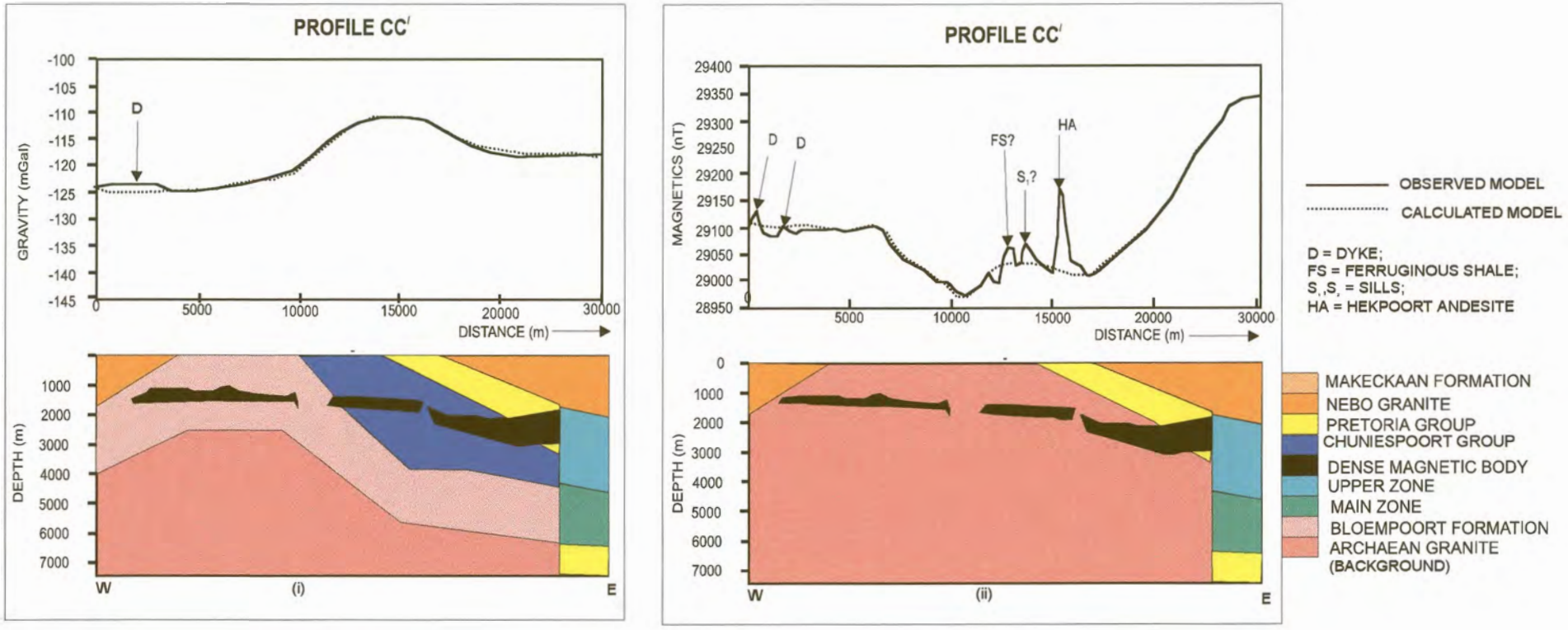

Figure 4.19c : Geophysical models for profiles CC' (i) the gravity and (ii) the magnetics

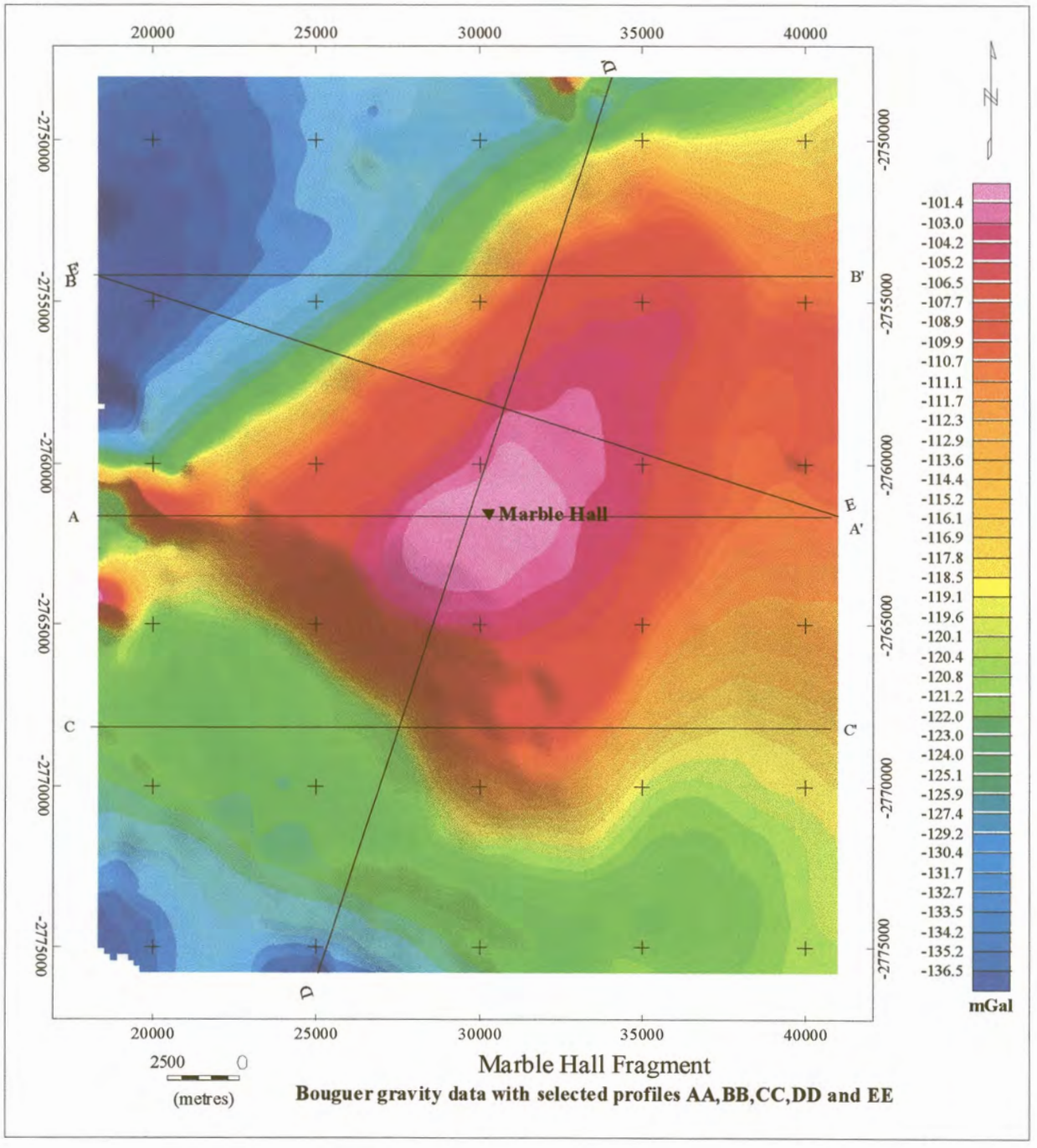

Figure 4.20a Gravity data showing the localities of profiles finally selected for 2.5-D modeling

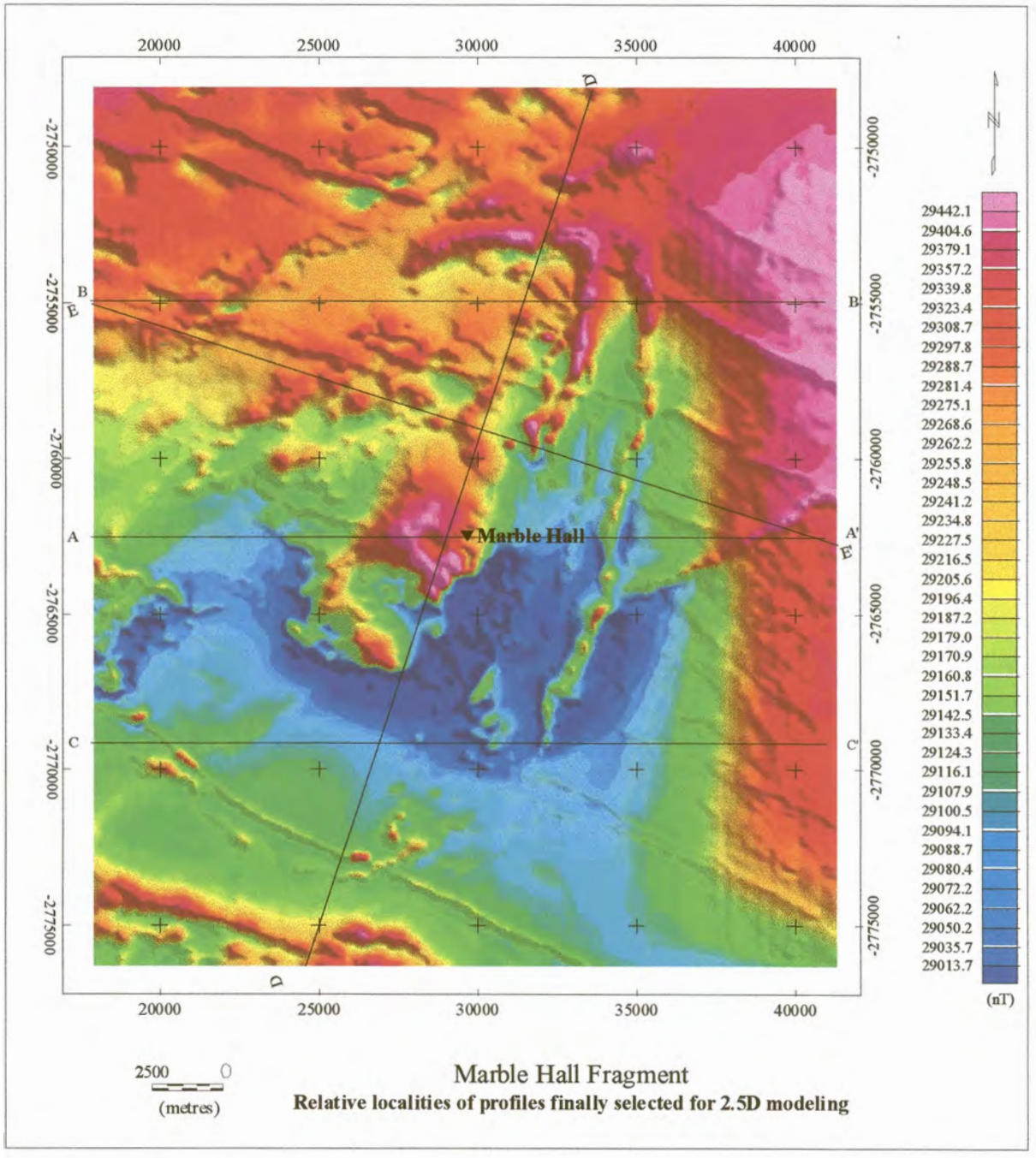

Figure 4.20b. Magnetic data showing the localities of profiles finally selected for 2.5-D modeling

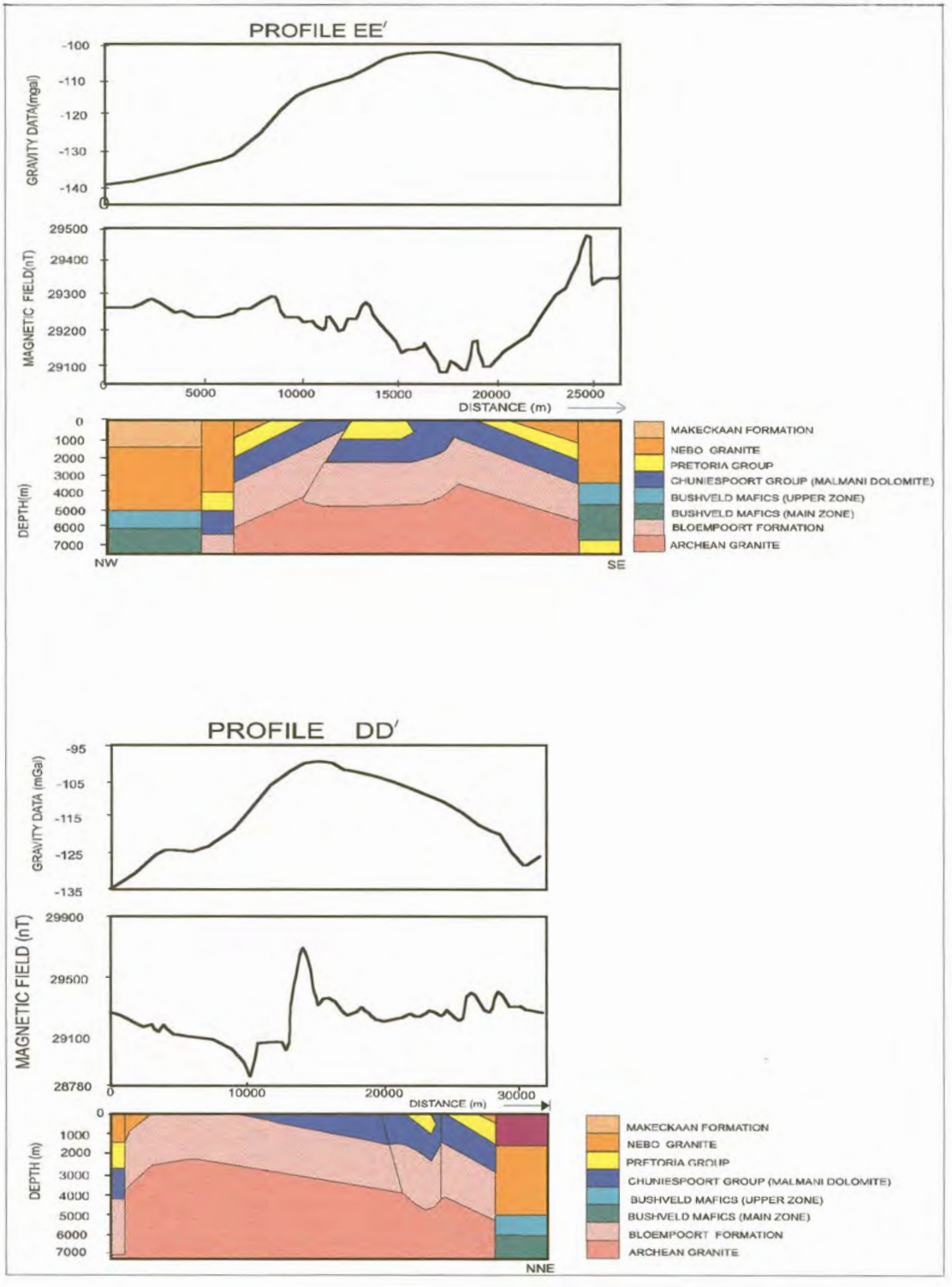

Figure 4.21 : Geological cross-sections gravity and magnetic data along profiles EE' and DD'.

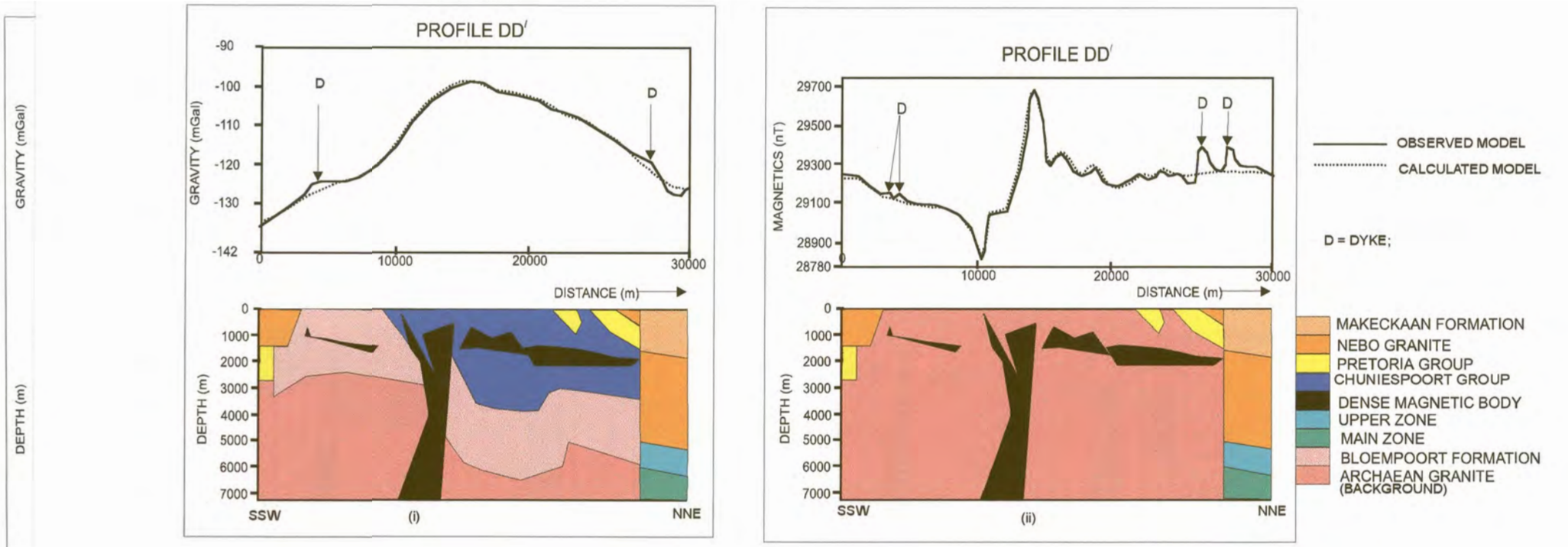

Figure 4.22: Geophysical models for profiles DD' (i) the gravity and (ii) the magnetics.

Fig

4.4.5. LIMITATIONS.

The process of quantitative interpretation of both gravity and magnetic anomalies endeavours to determine a source distribution whose anomalous field matches as closely as possible the actual field on the surface of measurement (Patterson and Reeves, 1985).
The interpretation is inherently ambiguous and this ambiguity arises because any given anomaly could be caused by an infinite number of possible sources. For example concentric spheres of constant mass but differing density and radius will all produce the same anomaly, since their mass acts as though located at the centre of the sphere. This ambiguity represents the inverse problem of potential field interpretation, which states that although the anomaly of a given body may be calculated uniquely, there are an infinite number of bodies that could give rise to any specified anomaly.

Another limitation to this interpretation is that a large deep body can also give the same anomaly as a small shallow body. This means that the amplitude and shape of an anomaly produced by a large body at great depth can be similar to that of a small body closer to the surface. In the same vein, a steeply dipping body and a vertical body might produce the same anomaly.

Removal of regional field to isolate the residual anomalies also provides a limitation in potential field interpretation especially in gravity surveying. This is because, if the regional field subtracted is too much, part of the residual anomalies of interest could be omitted and if too little a regional field is subtracted, fictitious residual anomalies could arise which are not supposed to be part of the anomalies of interest.

In this study, several samples of each particular rock type from surface outcrops have been

used for density determinations in order to obtain a reliable mean density and variance. In sedimentary rock sequences however, density tends to increase with depth due to compaction, and with age, due to progressive diagenesis, hence, non-availability of bore-hole information at depth from every part of the study area, might have an effect on the gravity models interpreted. A major consolation in this regard is that, the mean densities obtained for the different rock samples are compatible with that obtained in this area by Button (1973), Hattingh (1980), and Corner *et al.* (undated).

Due to non-uniqueness of potential field interpretation such as in the gravity and magnetic methods used in this study, constraints have been introduced in the form of simplification of geometry, limits to size or depth, range limits on density and susceptibility, location and extent of outcrops and other parameters seemed justifiable in the context of what is known or can be reasonably inferred about the Marble Hall geological environment.

4.5. CONCLUSIONS

Based on the data presented in the previous sections, the following conclusions can be made :

1. The high magnetic signature associated with the eastern limb of the Swartkop-Marble Hall Anticline, running from the south towards the north-east as observed on the total field map, is the surface expression of the Hekpoort Andesite Formation.

2. A well-defined fault, trending north-south, forms the eastern boundary of the Marble Hall Fragment. The dip of this fault could not be determined because there is no surface expression of the fault.

3. A highly magnetic, dense rock mass is situated in the centre of the Fragment. This rock mass is interpreted as an intrusive body with a central sub-vertical core section, surrounded at shallower levels, by sub-horizontal sill-like sections.

4. Due to non-uniqueness in potential field interpretation discussed above, the exact depth and thickness of the mafic sills cannot be categorically stated. It is conceivable that the sills might be thinner than indicated (Figures 4.19(a) and (b), 4.22, 4.23), but much closer to the surface.

5. The crescent shaped body with high magnetic signature along the axis of the Swartkop-Marble Hall Anticline and truncated by a fault to the north, is well defined but its origin is not obvious. The outcropping lithologies in that area can not explain the high magnetic signature. It is postulated that it might be a covered sill related to the Rustenburg Layered Suite.

6. Overall, the structure of the Marble Hall Fragment can be regarded as folded floor of Transvaal Supergroup rocks between two faults - the Wonderkop fault in the north-west and the delineated north-south trending fault in the east.

7. From model interpretations, it can be suggested that the intrusion of the Bushveld mafics post-dates the folding and perhaps some of the faults in the Fragment.

8. The dips of the faulting is given as vertical in this interpretation but it is conceivable that this might not be so.

Further investigation of the Marble Hall Fragment by other geophysical methods and finally drilling, will assist in confirming the presence and exact location in depth of the main intrusive mafic body which might have potential economic value.